# Best
# Available
# Copy

The ESC Public Affairs Office has reviewed this report, and it is releasable to the National Technical Information Service, where it will be available to the general public, including foreign nationals.

This technical report has been reviewed and is approved for publication.

FOR THE COMMANDER

Gary Tutungian
Administrative Contracting Officer
Contracted Support Management

MASSACHUSETTS INSTITUTE OF TECHNOLOGY
LINCOLN LABORATORY

# ADAPTIVE DETECTION AND COPY OF COHERENT NARROWBAND WAVEFORMS WITH UNCALIBRATED ARRAYS

*K.W. FORSYTHE*
*Group 44*

**TECHNICAL REPORT 994**

20 JUNE 1994

Approved for public release; distribution is unlimited.

DTIC QUALITY INSPECTED 3

**LEXINGTON**                                                    **MASSACHUSETTS**

# ABSTRACT

Adaptive detection and copy of temporally coherent narrowband waveforms with multiple sensors is discussed. Unlike related problems treated in the radar literature, the sensor response to the coherent signal of interest is assumed unknown. Thus the techniques presented can be used with uncalibrated sensor arrays. The signal processing takes advantage of the sensor array as well as the signal coherence in order to form an adaptive spatial beam that suppresses cochannel interference. More general signal models involving partial coherence are also considered.

# TABLE OF CONTENTS

# LIST OF ILLUSTRATIONS

# 1. INTRODUCTION

Adaptive detection and copy of temporally coherent (i.e., known) narrowband waveforms using multiple sensors has been treated extensively in the radar literature. Kelly [1] provides a maximum likelihood (ML) formulation of the problem (see also Kelly and Forsythe [2]). For radar problems, a fundamental assumption is that the sensor response to the signal of interest (SOI) is known. Variations on this assumption lead one to study the performance loss associated with imperfectly known sensor responses (wavefront mismatch).

In contrast, the problem of interest here is the detection and copy of a coherent waveform with a completely unknown wavefront. Lack of knowledge about the wavefront can be due to unresolved multipath or, more simply, to an uncalibrated (or uncalibratable) antenna array. The problem of wavefront mismatch is absent given the techniques discussed in this report, but for many applications there can be other problems associated with imperfect use of the coherent signal waveform (waveform mismatch). The impact of such problems is studied here. To make the techniques more concrete, a particular frequency domain application is discussed. For this application, the signal processing is called *frequency feature processing* (FFP).

In broad terms, the work presented here specializes the results of Kelly and Forsythe [2] to the problems of detection and copy of a coherent waveform with unknown wavefront. Specific forms of the detection statistic and adaptive beamformer are presented. These forms are suited to typical applications. Problems associated with waveform mismatch are addressed.

More specifically, Section 2.1 recalls the signal model of Kelly and Forsythe [2]. To simplify the exposition, the treatment of detection and copy in the body of this report is expressed in terms of a specific frequency domain application. However, the appendices provide a more general treatment. Section 2.2 expresses the *generalized likelihood ratio* detection statistic and copy weight of Kelly and Forsythe [2] for the signal model of interest. Section 3 reformulates the detection statistic and copy weight in forms more appropriate for applications. Section 4 discusses some difficulties with detection and copy in practical applications and quantifies performance.

1

# 2. DETECTION AND COPY STATISTICS

## 2.1 Signal Model

Let $Z = (Z(1), \ldots, Z(L))$ be an $N \times L$ array of vector samples of the output of an $N$ element antenna array. Each column of $Z$ represents, for FFP applications, a snapshot of the array output in a particular frequency cell. It is assumed below that these snapshots are independent. The entries of $Z$ are taken to be jointly complex circular Gaussian. A more general signal model is discussed in Appendix A.1.

One can partition the data $Z$ into the $N \times M$ subarray $Z_p$ (p-data) and the $N \times (L - M)$ subarray $Z_q$ (q-data): $Z = (Z_p \ Z_q)$. It is assumed that $L \geq M + N$. Each column of $Z$ is assumed to have the same covariance $R$. That is,

$$R = \mathrm{E}[(Z(k) - \mathrm{E}[Z(k)])(Z(k) - \mathrm{E}[Z(k)])^H]$$

where $\mathrm{E}[\cdot]$ denotes expectation. However, the modeled mean of $Z_q$ is assumed to be zero while that of $Z_p$ is

$$\mathrm{E}[Z_p] = \begin{cases} VA & \mathrm{H_S} \\ 0 & \mathrm{H_{NS}} \end{cases}$$

under the signal present ($\mathrm{H_S}$) and signal absent ($\mathrm{H_{NS}}$) hypotheses. $V$ is a $N \times J$ array, the columns of which represent the array responses (signal wavefronts) of $J$ emitters. $A$ is a $J \times M$ array of signal amplitudes.

The true mean of $Z$ need not agree with the model. It can be written in general as

$$\mathrm{E}[Z_p] = \mathcal{V}\mathcal{A}_p$$

$$\mathrm{E}[Z_q] = \mathcal{V}\mathcal{A}_q$$

where $\mathcal{A} = (\mathcal{A}_p \mathcal{A}_q)$ is a $J \times L$ array expressing contributions of the signal to both the p-data and q-data. $\mathcal{V}$ is a $N \times J$ array expressing the true array responses of $J$ emitters. When it is important to make a distinction, a script font is used to signify true properties of the signal mean as opposed to properties of the model (expressed in a roman font). Signal presence in the q-data is a form of model mismatch that impacts the detection and copy procedures described below.

For FFP applications (the treatment is more general in the appendices) $J = 1$. Then $\mathcal{A}$ is a vector representing the signal components in the p-data and q-data. Signal in the q-data is a type of modeling inaccuracy due, for example, to uncertainty in the signal bandwidth. For FFP

3

detection, $M = 1$ is assumed in addition. Then the modeled $A$ is a scalar that lives in one and only one frequency cell, which may or may not be known *a priori*.

The model of $V$ may vary considerably, leading to different forms of parameter estimators. $V$ is assumed to be completely unknown in the FFP applications. Thus the procedures described below can be used with uncalibrated arrays. Note that there is no modeling mismatch associated with $V$ in this case: all $V$'s are included in the model.

An example of a waveform amenable to FFP is a narrowband AM signal with significant energy in the carrier. For detection purposes, the signal is modeled as a pure tone at the carrier frequency. Thus detection suffers from model inaccuracies due to the true, multicell signal bandwidth. The effect of this modeling error is assessed in Section 4.2. Copy also relies on the tone model, but a guard band can be introduced to address the effects of an inaccurate model (see Section 4.3).

## 2.2 Maximum Likelihood Formulation

Letting $S \overset{\text{def}}{=} Z_q Z_q^H$, the generalized likelihood ratio (see Appendix A.2 for a concise description of the test in a more general situation as well as in the special case treated here) for deciding between the hypotheses $H_S$ and $H_{NS}$ is

$$\frac{V^H S^{-1} V}{V^H (ZZ^H)^{-1} V}. \tag{1}$$

The associated copy weight is expressed by

$$W = S^{-1} V (V^H S^{-1} V)^{-1}. \tag{2}$$

The expression $W^H Z_p$ provides a ML estimate of the signal amplitude $A$.

To complete the detection statistic and determine the copy weight $W$, Equation (1) must be maximized over $V$. $V$ can be modeled, for example, by a calibration table for the antenna array. Because detection and copy with uncalibrated arrays are of principal interest here, $V$ is assumed to be completely unknown. Thus Equation (1) must be maximized over all nonzero $V$. To do this, one can use the following well-known result, valid for any hermitian matrices $A$ and $B$, with $B$ positive definite.

$$\max_X \frac{X^H A X}{X^H B X} = \max_X \frac{X^H B^{-1/2} A B^{-1/2} X}{X^H X} = \lambda_{\max}(B^{-1/2} A B^{-1/2}) = \lambda_{\max}(B^{-1} A),$$

where the maximization occurs over vectors $X$ and $\lambda_{\max}(\cdot)$ denotes the largest eigenvalue of its argument. Let $e_{\max}(\cdot)$ denote the principal eigenvector of its argument. Then

$$X_{\max} = e_{\max}(B^{-1}A).$$

Applying the above fact to Equation (1), one has

$$\max_V \frac{V^H S^{-1} V}{V^H (ZZ^H)^{-1} V} = \lambda_{\max}[(S + Z_p Z_p^H)S^{-1}] = 1 + Z_p^H S^{-1} Z_p, \tag{3}$$

which occurs when

$$V_{\max} = e_{\max}[(S + Z_p Z_p^H)S^{-1}] = Z_p.$$

The copy weight associated with $V_{\max}$ is

$$W = S^{-1} Z_p (Z_p^H S^{-1} Z_p)^{-1}. \tag{4}$$

Detection based on Equation (3) enjoys a strong constant false alarm rate (CFAR) property. Specifically, the distribution of the detection statistic under $H_{\mathrm{NS}}$ does not depend on the spatial distribution of interference.

# 3. REFORMULATION OF DETECTION AND COPY

## 3.1 Detection

The detection and copy statistics presented above have more useful forms, especially when the frequency cell containing the SOI is not known but must be located as part of the detection procedure. The new statistics are derived by applying the Sherman-Morrison-Woodbury identity (see Golub and Van Loan [3])

$$(S + Z_p Z_p^H)^{-1} = S^{-1} - S^{-1} Z_p (1 + Z_p^H S^{-1} Z_p)^{-1} Z_p^H S^{-1}.$$

Consider detection first. The detection statistic is given by $Z_p^H S^{-1} Z_p$. This applies to a specific frequency cell. If the cell containing the SOI is not known. the covariance estimate (unnormalized) $S$ must be reformulated for each cell tested. However,

$$Z_p^H (Z Z^H)^{-1} Z_p = Z_p^H (S + Z_p Z_p^H)^{-1} Z_p = \frac{Z_p^H S^{-1} Z_p}{1 + Z_p^H S^{-1} Z_p}.$$

Because $x/(1 + x)$ is a monotonic increasing function, an equivalent form of the detection statistic is given by the left-hand-side of the above equation, namely

$$Z_p^H (Z Z^H)^{-1} Z_p. \tag{5}$$

This version of the statistic uses only one unnormalized covariance estimate $Z Z^H$ for all cells tested.

## 3.2 Copy

A similar (though less useful) reformulation is possible for the copy weight based on a particular cell:

$$
\begin{aligned}
(Z Z^H)^{-1} Z_p (Z_p^H (Z Z^H)^{-1} Z_p)^{-1} &= [S^{-1} Z_p (1 + Z_p^H S^{-1} Z_p)^{-1}] \\
&\quad \cdot [(Z_p^H S^{-1} Z_p)(1 + Z_p^H S^{-1} Z_p)^{-1}]^{-1} \\
&= S^{-1} Z_p (Z_p^H S^{-1} Z_p)^{-1}.
\end{aligned}
$$

The right-hand side of the above equation can be recognized as the adaptive copy weight introduced in Equation (4). Thus the adaptive weight can be written in the form

$$(Z Z^H)^{-1} Z_p (Z_p^H (Z Z^H)^{-1} Z_p)^{-1}. \tag{6}$$
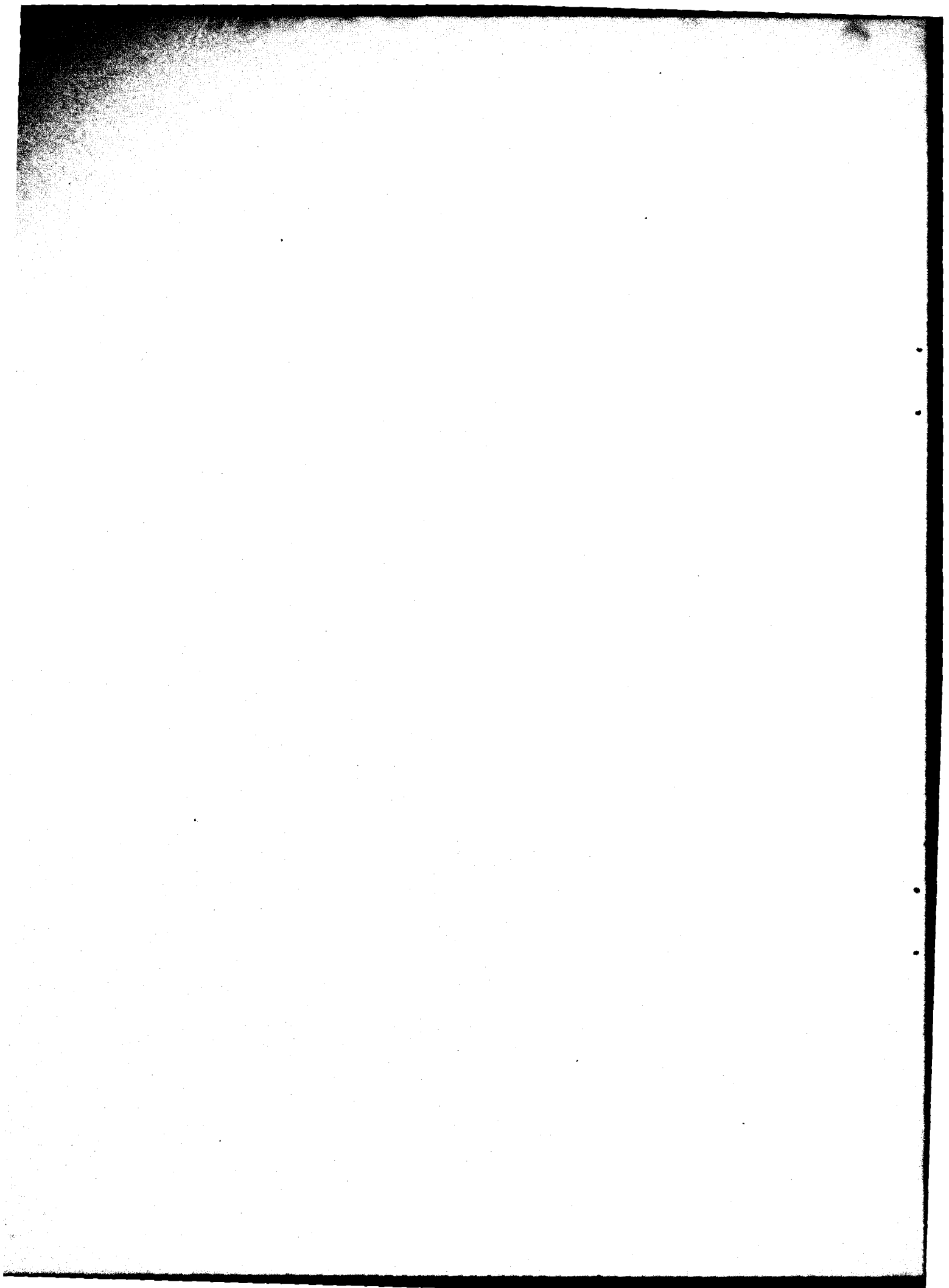
# 4. PERFORMANCE ASSESSMENT

Both the detection statistic of Equation (5) and copy weight of Equation (6) can suffer from modeling inaccuracies in practical applications. The signal model assumes that the SOI is concentrated in a single frequency cell while the interference, in principle, is found in all cells. Typical applications of FFP involve signals with spectral lines due to residual carriers or due to periodicities in the data. Thus a substantial fraction of the SOI power is concentrated in one or several cells, but there can be considerable signal power in other cells as well. In order to characterize performance, these modeling inaccuracies must be taken into account.

## 4.1 SNRs and Emitter Separations

Typically, the performance of adaptive array algorithms is assessed in terms of emitter levels and emitter separations. Some basic definitions of both are introduced next. More discussion of emitter separations is presented in Appendix C.

The *array signal-to-noise ratio* (ASNR) of an emitter in a background environment (noise and possibly some, but not all, interference) is the SNR at the output of an optimal beamformer. It is the largest SNR achievable with adaptive beamforming in the given environment. What constitutes the "background environment" as opposed to "interference" is largely a question of what is known as opposed to unknown. Because the background is often known, it is incorporated in the definition of ASNR because, in this case, the data can be prewhitened by the background before adaptive processing, which handles additional, unknown interference. In other words, it is useful to include any known background in the definition of ASNR in order to gauge performance against unknown (typically discrete) sources. In some cases it is convenient to exclude known interference from the concept of background environment. For example, the noise floor may be determined by spatially diffuse environmental sources rather than by thermal noise. Such a background, if it does not appear spatially white, can be suppressed to some extent by adaptive techniques. By excluding such interference from the definition of background, this suppression can be assessed [in terms of *array signal-to-interference ratio* (ASIR); see below]. However, it is worth noting that adaptive techniques provide the most benefit against discrete sources.

The calculation of ASNR is based on the covariance decomposition

$$R = \overbrace{R_S}^{\text{signal cov.}} + \underbrace{R_N}_{\text{background cov.}} .$$

In the following, the reader can safely assume $R_N = I_N$, where $I_N$ is the $N \times N$ identity matrix, representing a spatially white background. This leads to the most common definition of ASNR; but

9

as the discussion above indicates, other definitions can be useful. Adaptive beamforming maximizes the SNR at the output of the beamformer, forming

$$\max_{W} \frac{W^H R_S W}{W^H R_N W} = \lambda_{\max}(R_N^{-1} R_S),$$

which is achieved when

$$W_{\max} = e_{\max}(R_N^{-1} R_S).$$

Note that there is assumed to be no correlation between signal and background. In practice, $R_S = p_S V V^H$, expressing the contribution of a single coherent emitter to the total covariance. $V$ (a column vector here) is the emitter steering vector and $p_S$ is the emitter power. In this case,

$$\text{ASNR} = \lambda_{\max}(R_N^{-1} R_S) = p_S \lambda_{\max}(R_N^{-1/2} V V^H R_N^{-1/2}) = p_S(V^H R_N^{-1} V)$$

and

$$W_{\max} = R_N^{-1} V.$$

In an interference environment, the covariance is expressed by $R = R_S + R_I$, where $R_I \geq R_N$ is the contribution of interference sources (typically discrete) as well as the background environment. With the signal model discussed above, the optimal ASIR is given by $p_S(V^H R_I^{-1} V)$. This leads one to define the *interference induced loss*

$$\frac{V^H R_I^{-1} V}{V^H R_N^{-1} V}.$$

This is the loss of *signal-to-interference ratio* (SIR) due to the presence of the additional interference contained in $R_I$.

In a special case of interest, the added interference is due to a single coherent emitter, so that $R_I = R_N + p_I W W^H$, with $W$ the steering vector of the interferer. Define the separation in beamwidths between the two steering vectors $V$ and $W$ as

$$b \overset{\text{def}}{=} (2/\pi)\arcos(\frac{|V^H R_N^{-1} W|}{\|V\|_{R_N} \|W\|_{R_N}}) \tag{7}$$

where $\|V\|_{R_N} \stackrel{\text{def}}{=} (V^H R_N^{-1} V)^{1/2}$, etc. Appendix C explains this definition. When $R_N \propto I_N$, this definition agrees closely with the physical notion of beamwidth for values of $b$ less than one-half. Note that $b = 1$ corresponds to the orthogonality of vectors $V$ and $W$. Because (Sherman-Morrison-Woodbury again; see, for example, Golub and Van Loan [3])

$$R_I^{-1} = R_N^{-1} - \frac{p_I}{1 + p_I W^H R_N^{-1} W} R_N^{-1} W W^H R_N^{-1},$$

the interference induced loss becomes

$$1 - \frac{p_I W^H R_N^{-1} W}{1 + p_I W^H R_N^{-1} W} \cdot \frac{|V^H R_N^{-1} W|^2}{(W^H R_N^{-1} W)(V^H R_N^{-1} V)} \tag{8}$$

$$= 1 - \frac{\text{ASNR}_I}{1 + \text{ASNR}_I} \cdot \cos^2(\pi b/2), \tag{9}$$

where $\text{ASNR}_I$ is the ASNR of the interferer. As $\text{ASNR}_I$ increases, this expression reaches the asymptote $\sin^2(\pi b/2)$. Figure 1 shows some examples of the interference induced loss as a function of $\text{ASNR}_I$ and the beamwidth separation of the emitters. Note that an emitter separation of one-half beamwidth leads to a loss (the reciprocal of Equation (9) is plotted on dB scale, for convenience) of at most 3 dB. If, on the other hand, the emitters are within 0.1 beamwidths of each other, the loss can approach 16 dB.

Some additional comments on SIRs are necessary for the discussion below. The definition of ideal ASIR (when $J = 1$, $M$ arbitrary) can be *stated in terms of the signal model* of Section 2.1 using the terminology appropriate for FFP applications. A more general definition is given in the appendices.

Let $\mathcal{A}_k$, the $k$th component of $\mathcal{A}$, be the signal amplitude in the $k$th frequency cell, then the ideal ASIR becomes $\|\mathcal{A}\|^2 (V^H R^{-1} V)/L$. Note that this is really an average ideal ASIR taken over $L$ observations. This can also be called the p-data ideal ASIR when $\mathcal{A}_k = 0$ in the q-data. When there is SOI contamination of the q-data, one can define separate p-data and q-data ideal ASIRs by restricting $\|\mathcal{A}\|^2$ to the $p$ or $q$ components ($\|\mathcal{A}_p\|^2$ or $\|\mathcal{A}_q\|^2$).

There is a distinction between the ideal ASIR just defined, which is a per sample SIR, appropriate for characterizing copy performance, and the ideal *total* ASIR (TASIR), which is needed to characterize detection. The ideal TASIR, for FFP detection applications, is $L$ times the ideal ASIR. Recall that $L$ is the number of available samples. The ideal TASIR incorporates coherent and incoherent ($M > 1$) SOI integration into the SIR. For convenience, the ideal TASIR is called simply TASIR below.

## 4.2 Simulation Results: Detection

All the plots in this section are based on the TASIR (or sometimes the p-data and q-data versions).

Figure 2 shows the *cumulative distribution functions* (CDF) of the normalized detection statistic Equation (10) for SOI TASIRs of 10, 20, and 30 dB. The figure is based on a Monte Carlo simulation utilizing the statistical normal forms discussed in Appendix D.1. The dimensional parameters are $N = 4$, $M = 1$, and $L = 1000$. Also shown in the figure is the statistic with no signal present (false alarm statistic). Note that the detection statistics are essentially constant when the SOI TASIR is much larger than unity.

To see how the figures can be used, consider a signal with an ASNR of −4 dB that is 0.1 beamwidth away from a very strong interferer. Figure 1 shows that the interference induced loss is at most 16 dB. Thus the ideal ASIR is at least −20 dB. With $L = 1000$, the TASIR becomes 10 dB. The corresponding curve in Figure 2 can be used to determine detection performance. Note that the signal can be detectable even if the ASIR does not support good copy.

The false alarm probability can be characterized when $J = 1 = M$. See Appendix D.3.2 for the calculations and some simple approximations. Figure 3 shows false alarm probability for $N = 2, 4, 8, 16$ when $L$ is large. The normalized detection statistic of Equation (10) is used. Because Figure 3 shows a per look false alarm probability, very low values are displayed. The false alarm rate is independent of the spatial distribution of the interference. However, it does depend on the spectral distribution of the interference. If the interference is not spectrally flat, higher false alarm rates can result.

Appendix D.3 provides an approximation for the normalized detection statistic

$$\frac{L - M}{M} \lambda_{\max}[Z_p^H S^{-1} Z_p] \tag{10}$$

when $L \gg 1$. Assume $M = 1$, because this is the case of most interest for FFP applications. Let $\text{TASIR}_p$ denote the TASIR of the SOI in the p-data. Similarly, let $\text{TASIR}_q$ denote the TASIR of the SOI in the q-data. The detection statistic is essentially constant when $\text{TASIR}_p \gg 1$ and assumes the approximate value

$$L \frac{\text{TASIR}_p}{L + \text{TASIR}_q}. \tag{11}$$

When $\text{TASIR}_q \ll L$, the approximate value is $\text{TASIR}_p$. When $\text{TASIR}_q \gg L$, this value saturates at about $L\,\text{TASIR}_p/\text{TASIR}_q$. In either case, a significant peak in the statistic occurs at lines in the SOI spectrum because, in this case, the value of $\text{TASIR}_p/\text{TASIR}_q$ is comparable with unity and because $L$ is large.
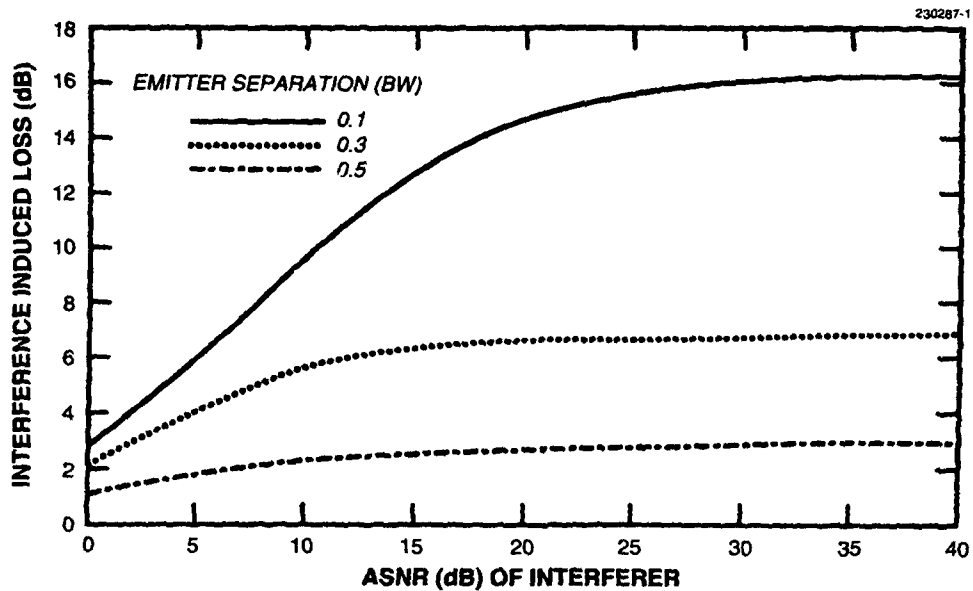
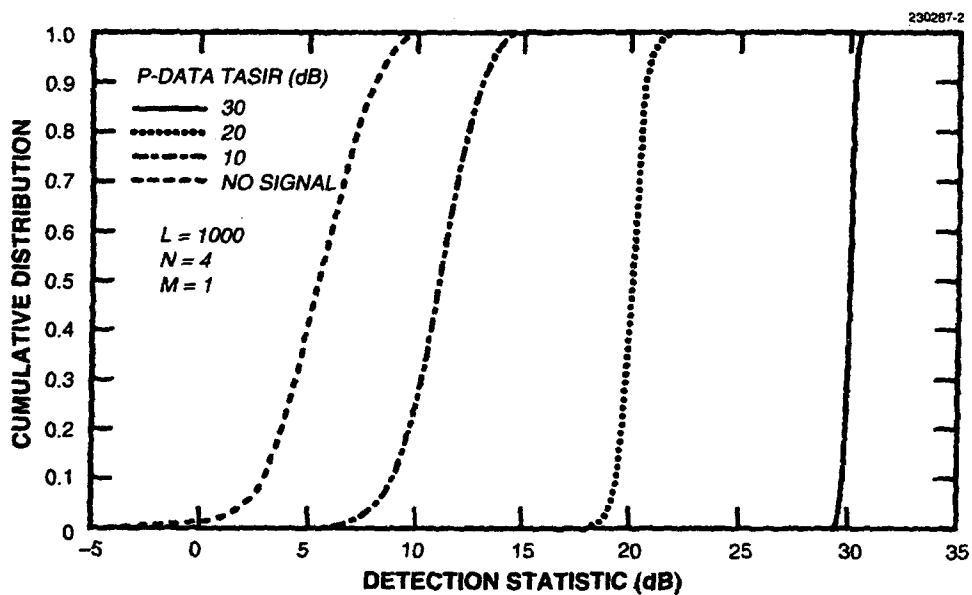*Figure 1.* *ASNR loss in cochannel interference.*



*Figure 2.* *Detection.*

13

Figure 4 is based on the same dimensional parameters as Figure 2. The SOI has a fixed (for each curve) TASIR of 30 dB in the p-data and TASIRs of 30, 20, and 10 dB in the q-data. Note that the SOI contamination of the q-data leads about a 3 dB loss in the detection statistic given 30 dB contamination, consistent with the approximations above. Contamination of 20 or 10 dB leads to little loss in detectability.

Similar comments apply to Figure 5 and Figure 6 where the p-data TASIR is reduced to 20 dB, the q-data TASIRs become 20, 10, and 0 dB, and the number of looks is 1000 (Figure 5) and 100 (Figure 6).

Finally, Figure 7 shows an SOI with 10 dB p-data TASIR and q-data TASIRs of 10, 0, and −10 dB. There are 1000 looks. Detectability suffers no essential loss.

## 4.3   Simulation Results: Copy

The copy performance achieved with the adaptive beamformer of Equation (4) is expressed in terms of the ASIR at the output of the copy beam. In Appendix D it is shown that this achieved ASIR (which is a random variable) has a distribution that depends only on the ideal ASIR and on the dimensional parameters $L$ and $N$ (recall, $M = 1$ in the applications discussed here). In other words, the achieved SIR depends on a particular scenario through the ideal ASIR. Scenario details such as interference spatial/polarization distributions are irrelevant to characterizing copy performance unless they alter the ideal ASIR.

Figure 8 shows the ideal and achieved ASIRs for a four element array using 100 samples. The vertical line in the figure indicates ideal ASIR, namely 10 dB. This line also represents the CDF of an ideal adaptive beamformer. The curved line shows the CDF of achieved ASIR (in dB) provided by FFP. The achieved ASIR is within a few tenths of a dB of the ideal. This is due to the large number of samples (100 here) typical of an FFP application with a consequent large coherent integration gain. In this example, the ideal TASIR is 30 dB.

When signal is present in the q-data, performance is degraded. As shown in Appendix D.4, the achieved ASIR depends only on the ideal ASIRs of the SOI in both the p-data and q-data, as well as on the dimensional parameters mentioned above. The next set of figures shows the performance degradation as a function of these ideal ASIRs. Each figure is based on a fixed ideal ASIR (shown in the caption) for the SOI in the p-data. The ideal ASIR of the SOI in the q-data is varied as indicated in the legend. The term "No Q-DATA" means that the signal lies only in the p-data. The dimensional parameters are varied as shown on the figures.

14

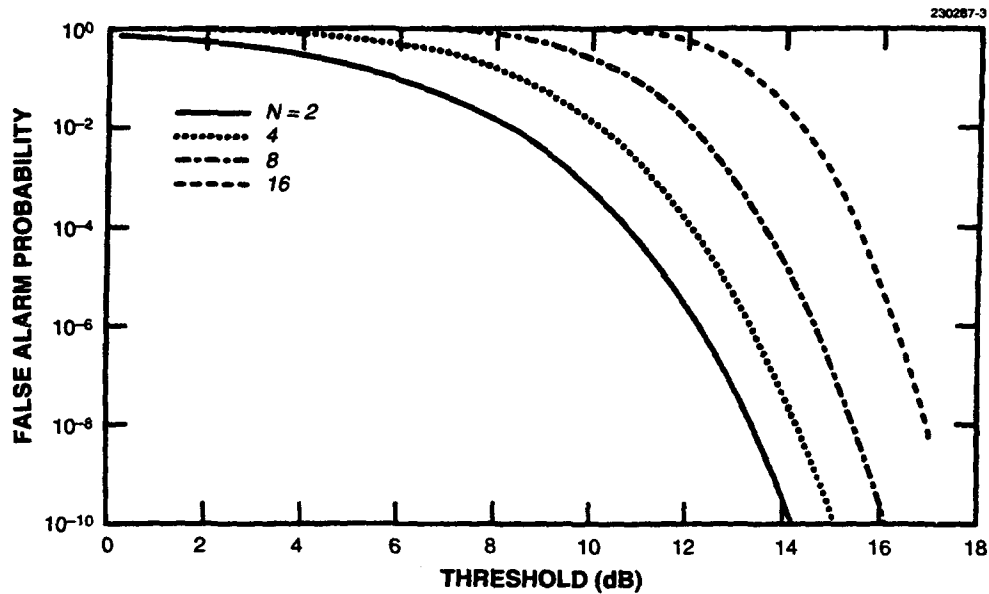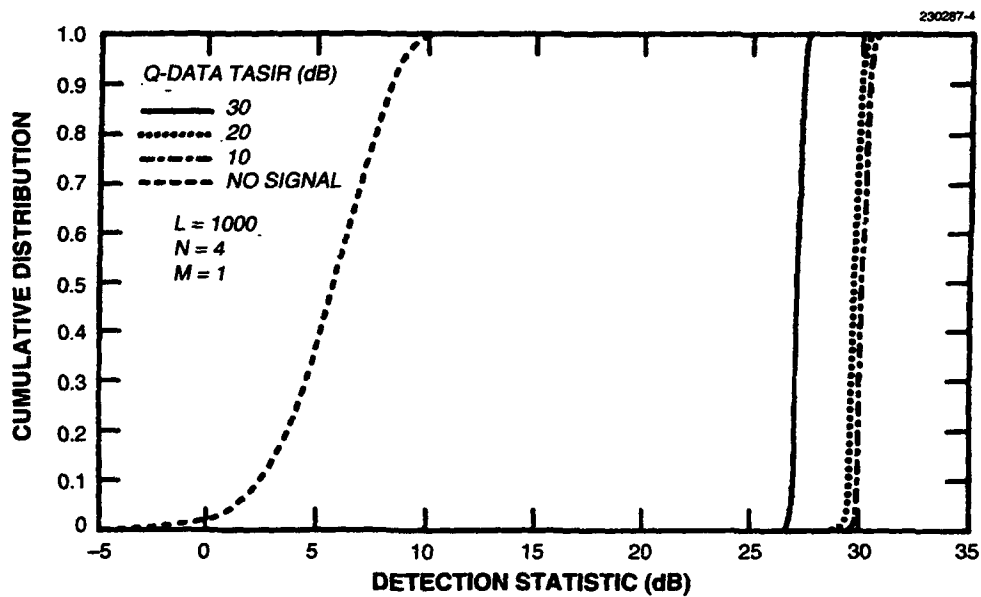Figure 3. False alarm probabilities $(L \gg N$ and $J = 1 = M)$.
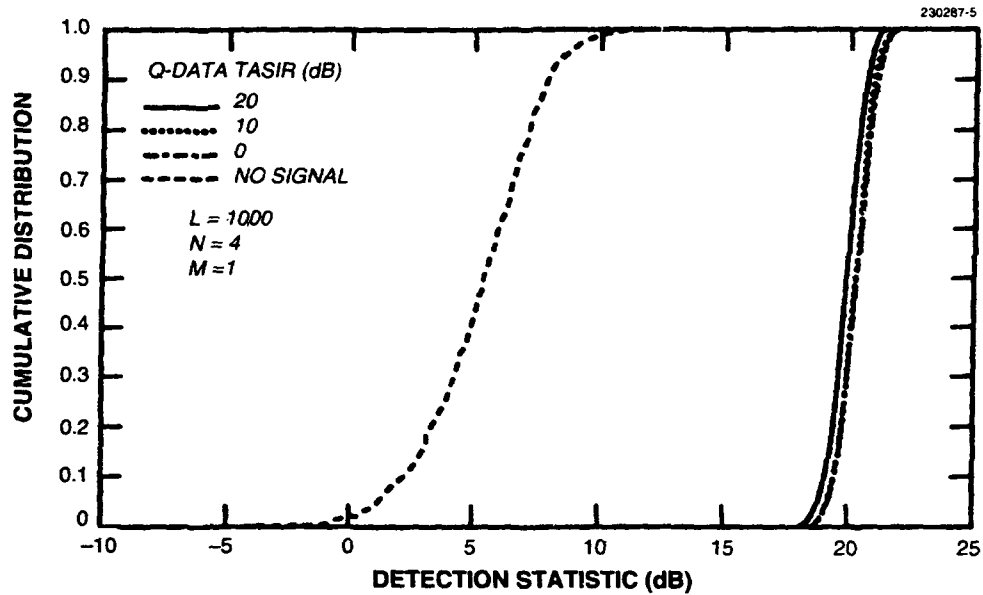


Figure 4. Detection with q-data contamination; p-data TASIR 30 dB.

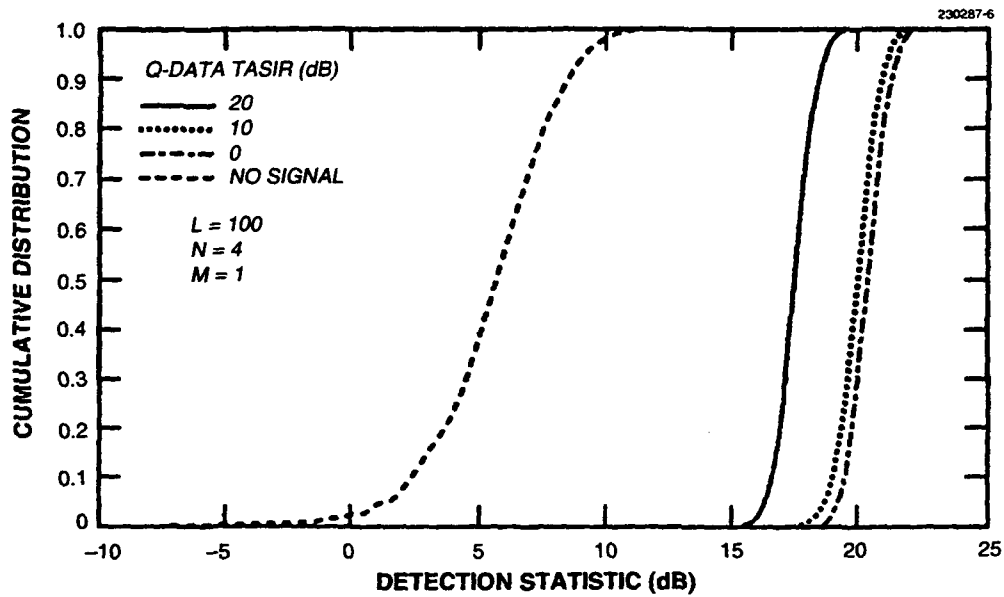Figure 5.   Detection with q-data contamination; p-data TASIR 20 dB.

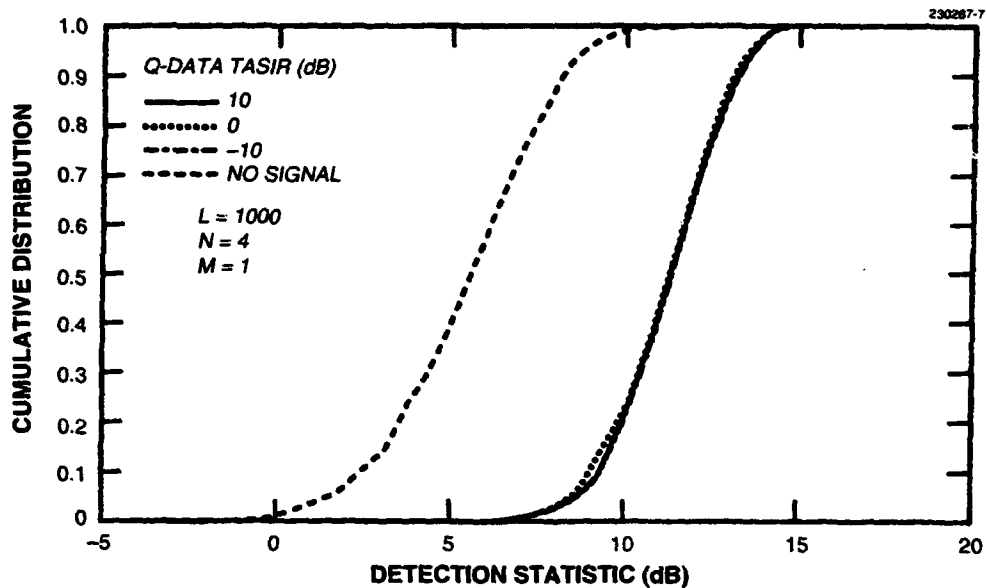Figure 6.   Detection with q-data contamination; p-data TASIR 20 dB.

16

230287-7

Figure 7.  Detection with q-data contamination; p-data TASIR 10 dB.
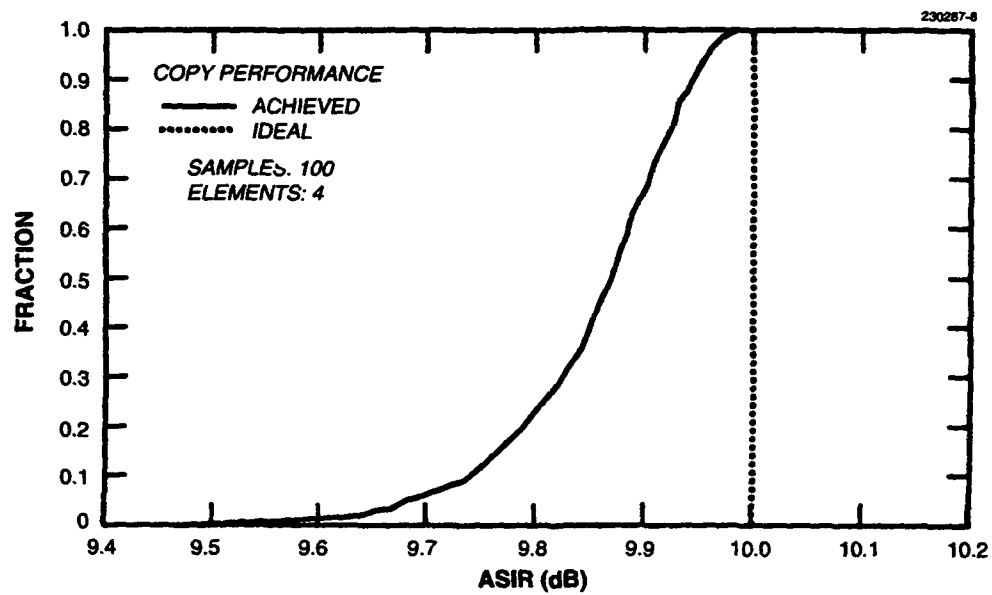


230287-8

Figure 8.  Achieved and ideal ASIRs.

17

The reader should note that the CDFs of achieved ASIR shown below are based on the p-data ideal ASIR. This is a convenient way to present the results given some of the processing options described below (i.e., guard bands). However, copy performance involving the p-data is not directly of interest because that component of the signal is already known upon detection and, hence, does not contain any additional information. It is more likely, but not necessary (see below), that the achieved ASIR of the q-data is of interest. In this case, the CDF curves should be translated by the difference (in dB) between the q-data and p-data ideal ASIRs. For example, a CDF curve of achieved ASIR based on an ideal p-data ASIR of 30 dB and an ideal q-data ASIR of 20 dB should be translated left by 10 dB.

Figure 9 shows that there is essentially no loss in achieved ASIR when $L \gg 1$ unless the q-data ASIR is much greater than the p-data ASIR. Here, the ideal p-data ASIR is low (10 dB). The loss due to q-data contamination increases as the number of looks $(L)$ is reduced (Figure 10) and as the p-data ideal ASIR is increased (Figure 11 and Figure 12). However, these losses are not significant as long as the q-data ASIR is much less than the p-data ASIR.

If, as mentioned above, the achieved ASIR for the q-data is of interest, one can rephrase the preceding statements. As long as the q-data ASIR is less than (approximately) the p-data ASIR, copy performance improves with increasing q-data ASIR (but fixed p-data ASIR). Once the q-data ASIR exceeds the p-data ASIR, copy performance degrades. For example, Figure 11 shows that a q-data ASIR of 20 dB leads to a median achieved ASIR (for the q-data) of about 18 dB. However, a q-data ASIR of 30 dB (which exceeds the p-data ASIR by 10 dB) leads to a median achieved ASIR of about 15 dB. In other words, copy performance has been degraded.

It is worth bearing in mind that the copy performance described in the figures is conditioned on detecting the SOI. When this is not possible with high probability, copy performance can deviate significantly from that shown in the figures due to mislocating the cell containing the SOI spectral line (for FFP applications). In the figures shown here only the 30 dB q-data curve of Figure 12 is effected.

It is possible for the SOI contamination of the q-data to have a more serious impact on performance. Figure 13 shows the effect of contamination at a high ideal ASIR. Figure 14 examines the same scenario with the addition of a 0.01 beamwidth mismatch between the SOI wavefront in the q-data and the p-data (which is taken to be truth). Note that the losses due to SOI contamination are considerably larger. Steering vector mismatch can arise for a number of reasons. For example, large multipath delays can cause wavefronts to vary across the signal bandwidth, violating the assumption that the SOI is narrowband.

18

**Figure 9.** *Copy with q-data contamination; p-data ASIR: 10 dB.*
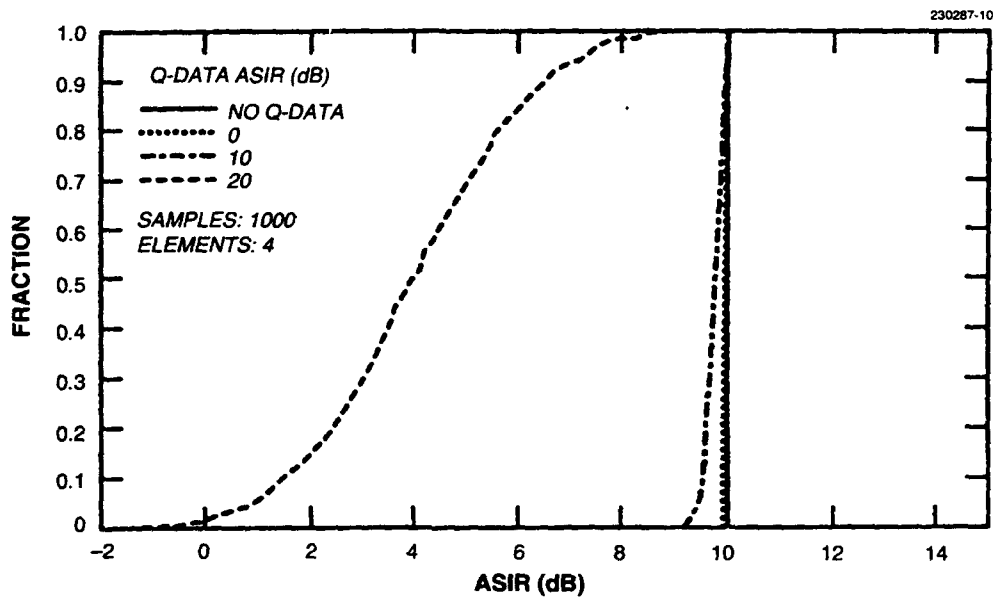
**Figure 10.** *Copy with q-data contamination; p-data ASIR: 10 dB.*

19

230287-11
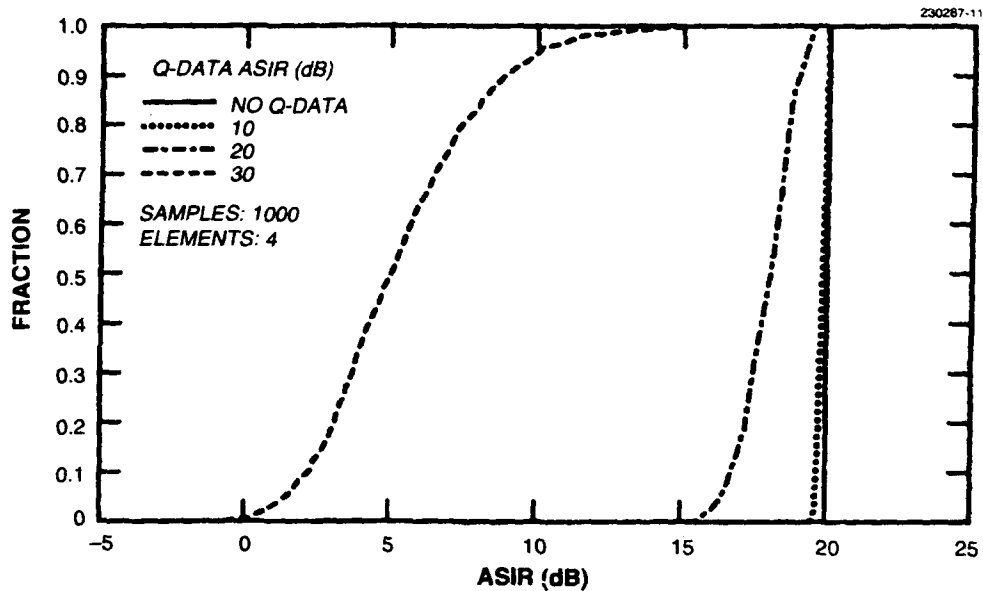
*Figure 11.   Copy with q-data contamination; p-data ASIR: 20 dB.*
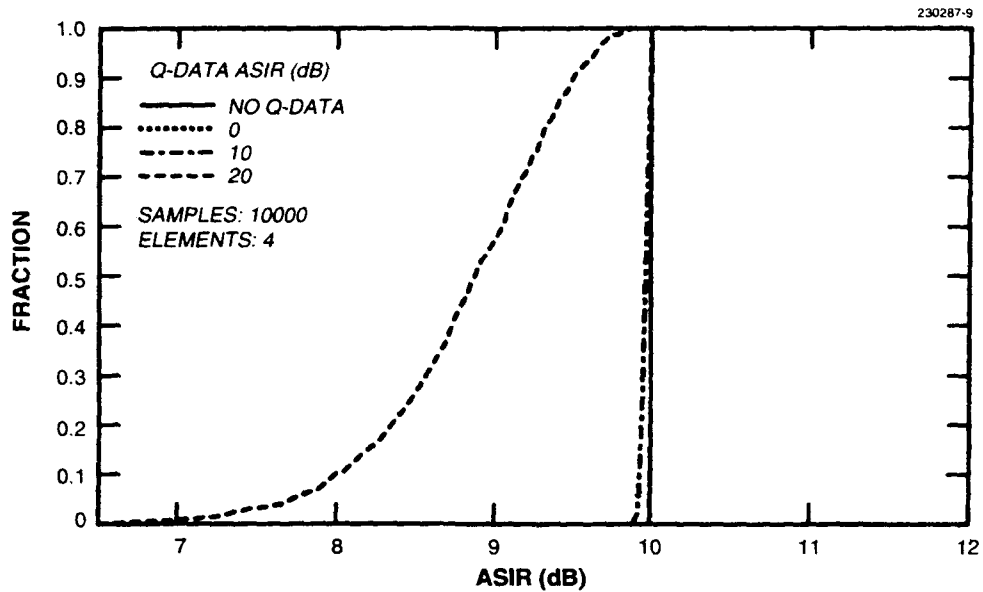


230287-12
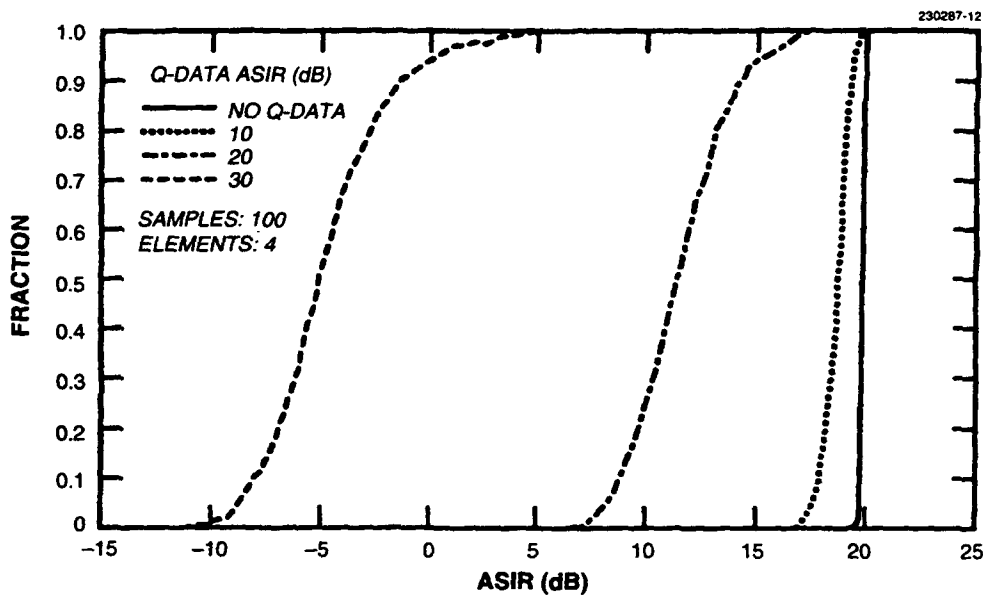
*Figure 12.   Copy with q-data contamination; p-data ASIR: 20 dB.*

20
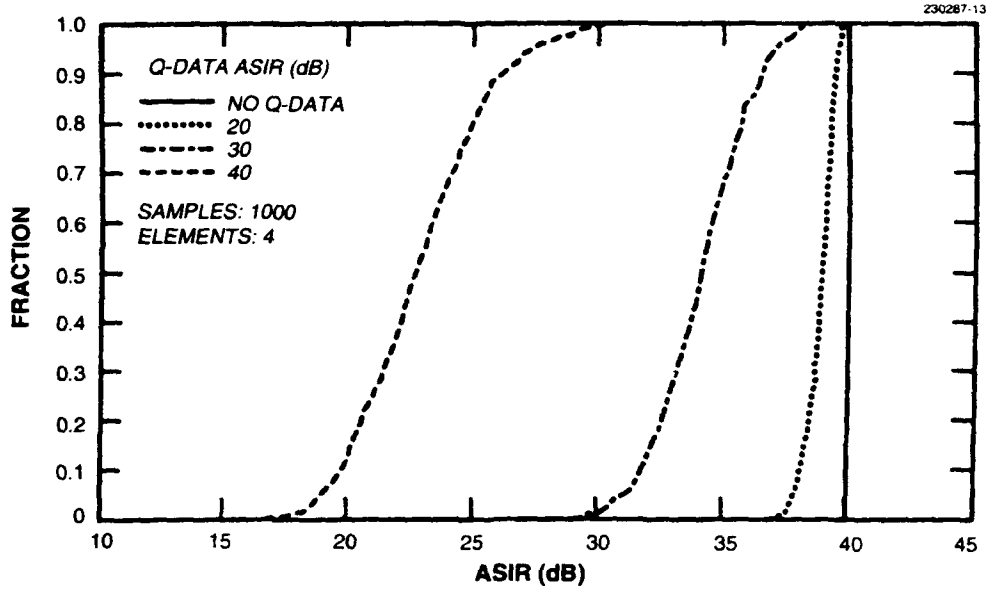
*Figure 13. Copy with q-data contamination; p-data ASIR: 40 dB.*
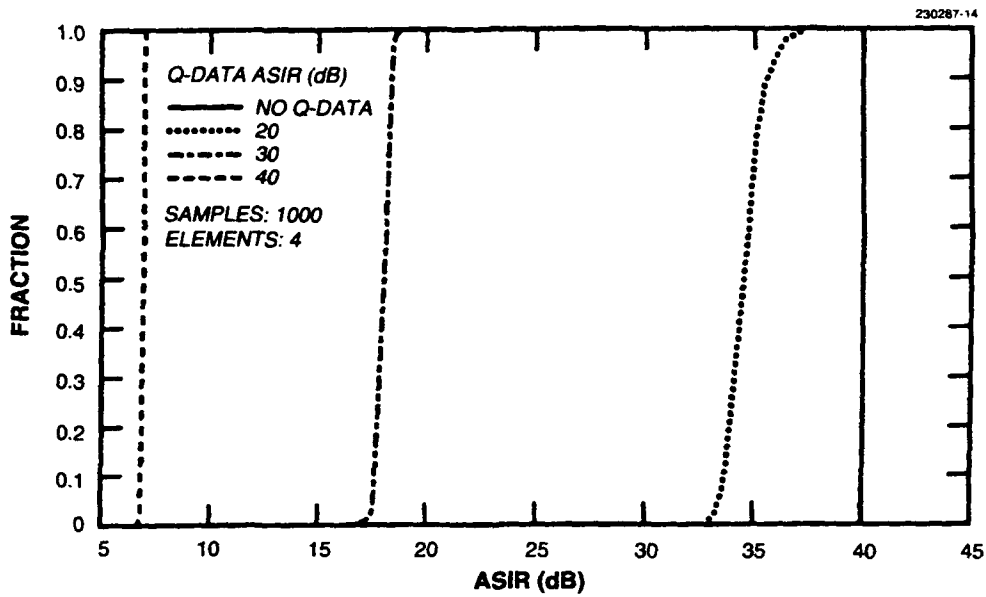


*Figure 14. Copy with q-data contamination and 0.01 beamwidth steering vector mismatch; p-data ASIR: 10 dB.*

21

For FFP applications, the q-data consists of all frequency cells ex pt the cell(s) containing the SOI lines. Thus the ideal ASIR in the q-data can be large. This could severely degrade copy performance, particularly when there is some wavefront variation over the band, as the figures indicate. To avoid this problem, a *guard band* can be centered about the line(s). One can think of preprocessing the data by notching out everything in the guard band, but allowing the line(s) to come through. The preprocessed data does not have significant SOI contamination in its q-data if the guard band is chosen appro ately. Of course, SOI power is thrown away (but only for weight determination) if the guard band is notched out. Instead, one can redefine the p-data so that it contains the guard band instead of just the line(s). However, if the line(s) contains a large fraction of the signal power, this will not improve performance significantly. Of course, if a guard band is used, the calculation of the q-data (instead of p-data) achieved ASIR described above must be modified.

# 5. SUMMARY

The work in Kelly and Forsythe [2] is reformulated and extended for applications involving the detection and copy of coherent waveforms with unknown wavefronts. An important application of this work (and a convenient example in the exposition) is called *frequency feature processing* (FFP). For this application, the waveforms are narrowband with significant power concentrated in one or several spectral lines. These waveforms have unknown wavefronts that differ from those of any cochannel interferers. The wavefront differences allow spatial nulling of the interference.

Detection and copy performance are discussed. Direction-finding is not considered because antenna calibration is assumed to be unavailable.

Detection enjoys a constant false alarm rate property such that the probability of false alarm does not depend on the spatial distribution of the environment, including interference. It must, of course, depend on the spectral distribution of the environment/interference. Detection performance relies on spatial nulling in addition to coherent integration of the signal of interest's (SOI) spectral line(s). As a result, signal detectability is substantially greater than that achievable with a discrete Fourier transform (DFT) alone.

A typical application involves a SOI with spectral line(s) (i.e., carrier or rate lines) in cochannel broadband (spectrally flat) interference. Because the SOI can have significant power outside of the lines, SOI self-nulling is a potential problem. Self-nulling can occur when the SOI signal level is large and most of the SOI power is not contained in the line(s). Loss of performance due to this problem is quantified.

The appendices discuss a more general signal model than that treated in the body of the report. Applications of this more general model are not pursued here.

23

# APPENDIX A
# STATISTICAL SIGNAL PROCESSING

The treatment in this appendix is more general than that in the body of the report. In particular, the signal model is much more elaborate. After recalling the maximum likelihood statistic in a form given in Kelly and Forsythe [2], some interesting reformulations are presented.

## A.1 Signal Model

Let $Z$ be an $N \times L$ array of vector samples of the output of an $N$ element antenna array. Each column of $Z$ is a snapshot of the array output at a particular time. It is assumed below that these snapshots are independent although the initial formulation is somewhat more general. The entries of $Z$ are taken to be jointly complex circular Gaussian with mean

$$E[Z] = VAT. \tag{A.1}$$

$V$ is a $N \times J$ array, the columns of which represent the array responses of $J$ emitters. $T$ is a $M \times L$ array, the rows of which can be interpreted as time domain basis waveforms. $A$ is a $J \times M$ array of signal amplitudes. In one case of interest here $M = 1$ and $J = 1$. Then $VAT$ expresses the time history of a single coherent waveform. In the formulation of hypothesis testing problems in Kelly and Forsythe [2], the $A$ array is assumed to be completely unknown. However, prior knowledge of $V$ and $T$ may vary considerably, leading to different forms of parameter estimators.

The covariance of $Z$ is given by

$$(\text{cov}(Z))_{(i,j);(k,l)} \stackrel{\text{def}}{=} E[(Z_{ij} - \overline{Z_{ij}})(Z_{kl} - \overline{Z_{kl}})^*] \tag{A.2}$$

where the overbar designates expected value and the $*$ denotes complex conjugate. It is often the case that the covariance has the special structure expressed by

$$\text{cov}(Z) = R \otimes C^* \tag{A.3}$$

where the Kronecker (tensor) product of matrices $A$ and $B$ is defined by

$$(A \otimes B)_{(i,j);(k,l)} \stackrel{\text{def}}{=} A_{ik} B_{jl} \tag{A.4}$$

25

The tensor product structure of the covariance can be interpreted as a factoring into spatial ($R$) and temporal ($C$) factors. For the applications of interest here, the factor $C$ is assumed to be known. It can express, for example, the time domain correlation imposed on a wideband waveform by the bandpass characteristic of a receiver.

## A.2 Maximum Likelihood Decision Statistic

Some additional notation and machinery is required. Consider data-independent matrices $F$ and $D$ that pre- and postmultiply the data, $Z$. $F$ can represent spatial processing of the data while $D$ can represent temporal processing. It is easy to show that

$$\mathrm{E}[FZD] = F\mathrm{E}[Z]D \tag{A.5}$$

and that (see Kelly and Forsythe [2], Equation A1-44)

$$\mathrm{cov}(FZD) = (FRF^H) \otimes (D^H CD)^\star. \tag{A.6}$$

In the following, it is assumed that $C = I_L$, the $L \times L$ identity matrix.

An orthonormal basis of the row space of $T$ can be chosen by defining

$$P = (TT^H)^{-1/2}T. \tag{A.7}$$

This is an $M \times L$ array, the rows of which span the same subspace as the rows of $T$. Furthermore, the rows of $P$ are orthonormal, that is

$$PP^H = I_M. \tag{A.8}$$

Choose a $K = L - M$ by $L$ array, $Q$, the rows of which are orthonormal and span the orthocomplement of the row space of $P$. The $P$ and $Q$ arrays have the following properties:

$$
\begin{aligned}
I_L &= P^H P + Q^H Q \\
PQ^H &= 0 \\
PP^H &= I_M \\
QQ^H &= I_K.
\end{aligned}
$$

Postmultiply the data array $Z$ with a data independent, unitary, $L \times L$ matrix, $U_L^H$, where

$$U_L = \begin{pmatrix} P \\ Q \end{pmatrix}. \tag{A.9}$$

Then

$$ZU_L^H = (ZP^H \ ZQ^H) \equiv (Z_p \ Z_q) \tag{A.10}$$

is a left-right partition of the transformed data. Postmultiplication by $U_L^H$ constitutes time-domain processing of the data array, $Z$, with a bank of orthogonal filters. The covariance machinery presented above tells us that

$$\operatorname{cov}(ZU_L^H) = R \otimes U_L I_L U_L^H = R \otimes I_L. \tag{A.11}$$

In order to find the *transformed mean* of $Z$, write

$$VAT = VBP \tag{A.12}$$

where

$$B \stackrel{\text{def}}{=} A(TT^H)^{1/2}. \tag{A.13}$$

Then

$$\mathrm{E}[Z_p] = VBPP^H = VB \ ; \ \mathrm{E}[Z_q] = VBPQ^H = 0. \tag{A.14}$$

Thus $Z_p$ and $Z_q$ are independent Gaussian arrays with independent columns and identical column (spatial) covariances. $Z_q$ has zero mean while $Z_p$ has a nonzero mean containing the signal parameters. Let $S \stackrel{\text{def}}{=} Z_q Z_q^H$ for use below. In addition, note that $ZZ^H = Z_p Z_p^H + S$.

From Kelly and Forsythe [2] (Equations 2-1, 2-2, 2-8, 2-57), the *generalized likelihood ratio* (GLR) decision statistic, maximized over $A$, can be written

$$\left( \frac{|V^H S^{-1} V|}{|V^H (ZZ^H)^{-1} V|} \right)^L = \frac{\max_{R,A} \pi^{-NL} |R|^{-L} e^{-\mathrm{tr} R^{-1} (Z - VAT)(Z - VAT)^H}}{\max_R \pi^{-NL} |R|^{-L} e^{-\mathrm{tr} R^{-1} ZZ^H}}, \qquad (A.15)$$

with the maximum likelihood (ML) estimate of $A$ given by (Kelly and Forsythe [2], Equation 2-49)

$$W^H Z T^H (TT^H)^{-1}$$

where

$$W \overset{\mathrm{def}}{=} S^{-1} V (V^H S^{-1} V)^{-1}.$$

For the special case treated in the body of the report,

$$T = (I_M \ 0_{M,L-M})$$

and hence $Z = (Z_p \ Z_q)$, so that

$$ZT^H (TT^H)^{-1} = (Z_p \ Z_q)(I_M \ 0_{M,L-M})^H = Z_p.$$

Thus the ML estimate of $A$ is $W^H Z_p$.

Let $\lambda_k(\cdot)$ denote the $k$th largest eigenvalue of its argument. In Kelly and Forsythe [2] Equation 2-61 it is shown that (see also Appendix B)

$$\max_V \frac{|V^H S^{-1} V|}{|V^H (ZZ^H)^{-1} V|} = \prod_{k=1}^J \lambda_k(S^{-1} ZZ^H) = \prod_{k=1}^J \lambda_k(I_N + S^{-1} Z_p Z_p^H)$$

$$= \prod_{k=1}^J (1 + \lambda_k(Z_p^H S^{-1} Z_p)). \qquad (A.16)$$

The last step follows from the fact that the nonzero characteristic values (including multiplicity, i.e., counting each occurrence of repeated values) of the products of any $n \times l$ $F$ and $l \times n$ $D$, namely $FD$ and $DF$, are the same. To see this, recall that the polynomial $|I_n + xC|$, for any square matrix $C$, has degree rank $C$ and has zeros of the form $-\lambda^{-1}$ where $\lambda$ runs over the nonzero characteristic values (roots of the characteristic polynomial) of $C$. In particular, if $C$ is diagonalizable, these characteristic values are the same as eigenvalues. From a determinant identity given in Appendix 1 (Equation A1-3) of Kelly and Forsythe [2], one has $|I_n + xFD| = |I_l + xDF|$, and hence FD and DF have the same nonzero characteristic values. In the application above, both $FD$ and $DF$ are diagonalizable and thus have the same nonzero eigenvalues.

28

The result above can be recast in a more useful form for applications. Using the Sherman-Morrison-Woodbury identity (see Golub and Van Loan [3]) one can write

$$
\begin{aligned}
Z_p^H (ZZ^H)^{-1} Z_p &= Z_p^H (S + Z_p Z_p^H)^{-1} Z_p \\
&= Z_p^H (S^{-1} - S^{-1} Z_p (I_M + Z_p^H S^{-1} Z_p)^{-1} Z_p^H S^{-1}) Z_p \\
&= (Z_p^H S^{-1} Z_p)(I_M + Z_p^H S^{-1} Z_p)^{-1}.
\end{aligned}
$$

Because $f(x) \overset{\text{def}}{=} x/(1+x)$ is monotonic increasing in $x$ for $x \geq 0$, it follows that

$$
\lambda_k(Z_p^H (ZZ^H)^{-1} Z_p) = \frac{\lambda_k(Z_p^H S^{-1} Z_p)}{1 + \lambda_k(Z_p^H S^{-1} Z_p)} \tag{A.17}
$$

and hence that

$$
1 + \lambda_k(Z_p^H S^{-1} Z_p) = (1 - \lambda_k(Z_p^H (ZZ^H)^{-1} Z_p))^{-1}. \tag{A.18}
$$

Thus

$$
\begin{aligned}
\max_V \frac{|V^H S^{-1} V|}{|V^H (ZZ^H)^{-1} V|} &= \prod_{k=1}^{J} (1 + \lambda_k(Z_p^H S^{-1} Z_p)) \\
&= \prod_{k=1}^{J} (1 - \lambda_k(Z_p^H (ZZ^H)^{-1} Z_p))^{-1}. \tag{A.19}
\end{aligned}
$$

When $J = M$ this becomes

$$
|I_M - Z_p^H (ZZ^H)^{-1} Z_p|^{-1}. \tag{A.20}
$$

## A.3 Special Case: $J = 1 = M$

With $P_Z \overset{\text{def}}{=} Z^H (ZZ^H)^{-1} Z$ and $J = 1$, the detection test statistic Equation (A.19) becomes

$$
(1 - \lambda_{\max}(Z_p^H (ZZ^H)^{-1} Z_p))^{-1} = (1 - \lambda_{\max}(P P_Z P^H))^{-1}. \tag{A.21}
$$

With $M = 1$ this is just

$$(1 - \|PP_Z\|^2)^{-1}.$$

Thus, if $P$ varies over a parameterized family of waveforms, the GLR detection test involves maximizing

$$\|PP_Z\|^2 = \frac{TP_ZT^H}{TT^H} \tag{A.22}$$

This can be viewed as minimizing the angle between the waveform, $T$, and the row space of the observations, $Z$.

# APPENDIX B
## A MAXIMIZATION PROBLEM

Consider maximizing the determinant ratio

$$\max_X \frac{|X^H A X|}{|X^H B X|} \tag{B.1}$$

over all full rank $N \times J$ matrices $X$ ($J \leq \text{rank}(A)$). $A$ and $B$ are both hermitian positive semi-definite and in addition $B > 0$. Then

$$\max_X \frac{|X^H A X|}{|X^H B X|} = \max_X \frac{|X^H B^{-1/2} A B^{-1/2} X|}{|X^H X|}$$

$$= \max_X \frac{|(X(X^H X)^{-1/2})^H B^{-1/2} A B^{-1/2} (X(X^H X)^{-1/2})|}{|(X(X^H X)^{-1/2})^H (X(X^H X)^{-1/2})|}$$

$$= \max_{\mathcal{E}} |\mathcal{E}^H B^{-1/2} A B^{-1/2} \mathcal{E}|$$

$$= \prod_{k=1}^J \lambda_k(B^{-1/2} A B^{-1/2}) = \prod_{k=1}^J \lambda_k(B^{-1} A)$$

where $\mathcal{E}$ runs over $N \times J$ arrays with orthonormal columns (that is, satisfying $\mathcal{E}^H \mathcal{E} = I_J$). The second to last equality is well-known (see, for example, Bellman [4], p. 129). This inequality can also be viewed as a consequence of the stronger result (Poincaré separation theorem)

$$\lambda_k(B^{-1/2} A B^{-1/2}) \geq \lambda_k(\mathcal{E}^H B^{-1/2} A B^{-1/2} \mathcal{E})$$

found, for example, in Horn and Johnson [5]. Letting $e_J(\cdot)$ denote the $N \times J$ matrix, the columns of which are the top $J$ eigenvectors of its argument, the maximum occurs when $X = e_J(B^{-1} A)\Gamma$, where $\Gamma$ is an arbitrary nonsingular $J \times J$ array.

# APPENDIX C
# ARRAY BEAMSHAPES

The angle $b$ of Equation (7) is fundamental in the geometrical interpretation of signal processing. Mathematically, $b$ is proportional to the geodesic distance between the two array responses $R_N^{-1/2}V$ and $R_N^{-1/2}W$, interpreted as points in projective space. Note that $b$ has been normalized so that $b = 1$ corresponds to orthogonal array responses in the noise-whitened coordinates. To make physical sense of this definition, consider the important special case in which $R_N \propto I_N$.

Some new notation is required. For the most part, the notation in this section is not used in the rest of the report and any conflicts should be ignored. Let $V(\theta, \phi)$ be the array response parameterized by zenith angle (complement of elevation) $\theta$ and azimuth angle $\phi$. A convenient coordinate system is provided by the unit direction-of-arrival vectors $u(\theta, \phi)$:

$$u(\theta, \phi) \stackrel{\text{def}}{=} (\sin(\theta)\cos(\phi), \sin(\theta)\sin(\phi), \cos(\theta))^T$$

For arrays with perfectly matched element patterns (a common modeling assumption), the response of the $k$th element can be written ($V = (v_1, \ldots, v_N)^T$)

$$v_k(\theta, \phi) = g(\theta, \phi)e^{i\frac{2\pi}{\lambda}d_k^T u(\theta, \phi)}$$

where $d_k$ is the three-dimensional location of the $k$th antenna element and $g(\theta, \phi)$ is the antenna pattern common to all elements. Let

$$u_\Delta \stackrel{\text{def}}{=} u(\theta_1, \phi_1) - u(\theta_2, \phi_2).$$

Armed with this notation, one has the approximation ($b \ll 1$)

$$1 - \frac{\pi^2}{4}b(\theta, \phi)^2 \approx \cos^2(\frac{\pi}{2}b(\theta, \phi)) = \frac{|V^H(\theta_2, \phi_2)V(\theta_1, \phi_1)|^2}{\|V(\theta_1, \phi_1)\|^2 \|V(\theta_2, \phi_2)\|^2}$$

$$\approx 1 - \left(\frac{2\pi}{\lambda}\right)^2 u_\Delta^T(D - dd^T)u_\Delta$$

where

$$D \stackrel{\text{def}}{=} N^{-1} \sum_{k=1}^{N} d_k d_k^T$$

and

$$d \stackrel{\text{def}}{=} N^{-1} \sum_{k=1}^{N} d_k.$$

Thus an approximate expression for $b$ becomes

$$b^2 \approx \frac{16}{\lambda^2} u_\Delta^T (D - dd^T) u_\Delta.$$

When $u_\Delta$ is small, this expression indicates that the array responses at angle $b$ from a fixed array response $V(\theta_2, \phi_2)$ form an ellipse (planar arrays) in $(u_x, u_y)$ space. Furthermore, this ellipse has the same shape no matter what point of reference $V(\theta_2, \phi_2)$ is used. By extrapolating this expression out to $b = 1$ [where the array responses $V(\theta_1, \phi_1)$ and $V(\theta_2, \phi_2)$ would be orthogonal if the approximation held] one has the definition of beamshape:

$$1 = \frac{16}{\lambda^2} u_\Delta^T (D - dd^T) u_\Delta. \tag{C.1}$$

This equation is motivated by a peak-to-null definition of beamwidth. As mentioned above, the normalization of $b$ is chosen so that $b = 1$ corresponds to a null (orthogonality) in the pattern.

For planar arrays, Equation (C.1) describes an ellipse in $(u_x, u_y)$ coordinates with major and minor semiaxes given by

$$\frac{\lambda}{4} \cdot \lambda_{\min}^{-1/2}(D - dd^T) \text{ and } \frac{\lambda}{4} \cdot \lambda_{\max}^{-1/2}(D - dd^T).$$

Equation (C.1) can be applied to arbitrary array geometries to yield a physical beam. For example, a completely filled (sampled arbitrarily finely) line array of length $A$ has a beam of size $\sqrt{3/4} \cdot \lambda/A$. A filled (including interior) circular array of diameter $A$ has a circular beamshape of radius $\lambda/A$. In all cases, the beam size is related to $\lambda/A$ where $A$ is a characteristic size of the array. Similar beamshapes can be motivated by Cramèr-Rao bounds on direction-finding (see Delong [6]).

34

# APPENDIX D
# PERFORMANCE

It is difficult to characterize analytically the statistical performance of the tests described above, at least in the general case. However, some simple coordinate transformations allow these statistics to be cast in simpler forms that depend on a reduced set of parameters. These *normal forms* can be the first step in an analytical characterization of performance, but they also can be used as the basis of Monte-Carlo evaluations. For the most part, this is the approach taken here.

## D.1 Normal Forms

Let the data $Z$ have covariance $R \otimes I_L$, as above, but let the mean of $Z$ be $\mathcal{V}\mathcal{A}\mathcal{T}$ instead of the expected $VAT$. Here, $\mathcal{A}$ is $J \times \mathcal{M}$ (instead of $J \times M$) and $\mathcal{T}$ is $\mathcal{M} \times L$ (instead of $M \times L$). This models a mismatch between the expected signal structure and the true structure. $\mathcal{V}$ has the same dimensionality $N \times J$, but represents a specific value of $V$ below. Choose a unitary $U$ so that

$$U R^{-1/2} \mathcal{V} (\mathcal{V}^H R^{-1} \mathcal{V})^{-1/2} = E_J = (e_1, \dots, e_J)$$

where $e_k$ is the column vector of length $N$ with all zero entries with the exception of a single one in the $k$th entry. Define $\mathcal{Z} \stackrel{\text{def}}{=} U R^{-1/2} Z$. Consider the partitioning

$$(\mathcal{Z}_p \ \mathcal{Z}_q) = \mathcal{Z} \begin{pmatrix} P \\ Q \end{pmatrix}^H = (U R^{-1/2} Z_p \ U R^{-1/2} Z_q).$$

The covariances of these new variables are

$$\text{cov}(\mathcal{Z}) = I_N \otimes I_L$$
$$\text{cov}(\mathcal{Z}_p) = I_N \otimes I_M$$
$$\text{cov}(\mathcal{Z}_q) = I_N \otimes I_{L-M}.$$

It is convenient to introduce some notation to describe their means. Define

$$\mathcal{B} \stackrel{\text{def}}{=} (\mathcal{V}^H R^{-1} \mathcal{V})^{1/2} \mathcal{A} (\mathcal{T} \mathcal{T}^H)^{1/2}$$
$$\mathcal{C} \stackrel{\text{def}}{=} \mathcal{B} (\mathcal{T} \mathcal{T}^H)^{-1/2} \mathcal{T} P^H$$
$$\mathcal{D} \stackrel{\text{def}}{=} \mathcal{B} (\mathcal{T} \mathcal{T}^H)^{-1/2} \mathcal{T} Q^H.$$

Then the means of the new variables are

$$E[\mathcal{Z}_p] = E_J C$$
$$E[\mathcal{Z}_q] = E_J D.$$

## D.2 Detection

The detection statistic can be expressed equivalently through the top $J$ eigenvalues of

$$Z_p^H S^{-1} Z_p \qquad (D.1)$$

This form is convenient for characterizing detection performance. Define $\mathcal{S} \stackrel{\text{def}}{=} \mathcal{Z}_q \mathcal{Z}_q^H$. In terms of the new random variables, one can write

$$\mathcal{Z}_p^H S^{-1} \mathcal{Z}_p = (U R^{-1/2} Z_p)^H [(U R^{-1/2} Z_q)(U R^{-1/2} Z_q)^H]^{-1}(U R^{-1/2} Z_p) = Z_p^H S^{-1} Z_p.$$

Thus the detection statistic can be expressed in a normal form that does not involve the scenario parameters other than through the new parameters $C$ and $D$.

One can replace $\mathcal{Z}$ with

$$\mathcal{Z} \begin{pmatrix} P \\ Q \end{pmatrix}^H \begin{pmatrix} U_M & 0 \\ 0 & U_{L-M} \end{pmatrix} \begin{pmatrix} P \\ Q \end{pmatrix}$$

where $U_M$ and $U_{L-M}$ are unitaries. This causes $\mathcal{Z}_p$ to be replaced by $\mathcal{Z}_p U_M$ and $\mathcal{Z}_q$ by $\mathcal{Z}_q U_{L-M}$. The detection statistic (depending only on eigenvalues) is unchanged. However, the p-mean becomes $E_J C U_M$ while the q-mean becomes $E_J D U_{L-M}$. Thus detection depends only on the values of $CC^H$ and $DD^H$. These values are determined next.

Define

$$\Gamma \stackrel{\text{def}}{=} (TT^H)^{-1/2}(TT^H)(TT^H)^{-1/2}$$

so that

$$CC^H = \mathcal{B}\Gamma\Gamma^H\mathcal{B}^H$$
$$DD^H = \mathcal{B}(I_\mathcal{M} - \Gamma\Gamma^H)\mathcal{B}^H = \mathcal{B}\mathcal{B}^H - CC^H.$$

Note that

$$CC^H = (\mathcal{V}^H R^{-1} \mathcal{V})^{1/2} [\mathcal{AT} (T^H(TT^H)^{-1}T) T^H \mathcal{A}^H] (\mathcal{V}^H R^{-1} \mathcal{V})^{1/2} \tag{D.2}$$

$$\leq (\mathcal{V}^H R^{-1} \mathcal{V})^{1/2} (\mathcal{A}TT^H\mathcal{A}^H) (\mathcal{V}^H R^{-1} \mathcal{V})^{1/2} = \mathcal{BB}^H \tag{D.3}$$

with equality when $M = \mathcal{M}$ and $T = \mathcal{T}$. In addition

$$DD^H = (\mathcal{V}^H R^{-1} \mathcal{V})^{1/2} [\mathcal{AT} (I_L - T^H(TT^H)^{-1}T) T^H \mathcal{A}^H] (\mathcal{V}^H R^{-1} \mathcal{V})^{1/2}$$

$$\leq (\mathcal{V}^H R^{-1} \mathcal{V})^{1/2} (\mathcal{A}TT^H\mathcal{A}^H) (\mathcal{V}^H R^{-1} \mathcal{V})^{1/2} = \mathcal{BB}^H.$$

Detection performance depends only on the dimensional parameters $(N, L, M, J, \mathcal{M})$, the normalized signal level $\mathcal{B}$, and the mismatch expressed, for example, by $\Gamma\Gamma^H$.

When there is no mismatch (i.e., $M = \mathcal{M}$ and $T = \mathcal{T}$), one can show that the detection statistic depends only on the eigenvalues of $CC^H$ (see also Kelly and Forsythe [2]). To show this, let the $N \times N$ unitary $\mathcal{U}$ be defined so that

$$\mathcal{U} = \begin{pmatrix} \mathcal{U}_J & 0 \\ 0 & I_{N-J} \end{pmatrix}.$$

Consider changing random variables: $\mathcal{Z} \mapsto \mathcal{UZ}$. The detection statistic is based on the top $J$ eigenvalues of

$$\mathcal{S}^{-1} \mathcal{Z}_p \mathcal{Z}_p^H \mapsto \mathcal{U} \mathcal{S}^{-1} \mathcal{Z}_p \mathcal{Z}_p^H \mathcal{U}^H$$

and hence is unchanged. The covariance of $\mathcal{Z}$ is also unchanged. However, the p-mean and q-mean of $\mathcal{Z}$ are altered:

$$\mathrm{E}[\mathcal{UZ}_p] = \mathcal{U}E_J C = E_J \mathcal{U}_J C$$

$$\mathrm{E}[\mathcal{UZ}_q] = \mathcal{U}E_J D = E_J \mathcal{U}_J D = 0.$$

Thus the detection statistic depends only on $\mathcal{U}_J CC^H \mathcal{U}_J^H$ for arbitrary $\mathcal{U}_J$, and hence it depends on the eigenvalues of $CC^H$, which are, from Equation (D.3), the eigenvalues of $\mathcal{BB}^H$, namely, those of

$$(\mathcal{V}^H R^{-1} \mathcal{V})(\mathcal{A}TT^H\mathcal{A}^H). \tag{D.4}$$

When $J = 1$, this is a scalar called the ideal *total array signal-to-interference ratio* (TASIR).

## D.3 Special Case

For an application such as frequency feature processing (FFP), as discussed in the body of the text, consider the special case when $J = 1$, $M = \text{card}(C)$, $\mathcal{M} = L$, $T$ is unitary, and $T = T_C$, the array formed from a subset $C$ of rows from $T$. Note that card$(\cdot)$ counts the number of elements in a set. The rows of $T$ can represent any orthonormal signal basis (e.g., Fourier components or wavelets) with the signal of interest (SOI) concentrated in a particular subspace (i.e., subband or time-frequency cell).

Let $\mathcal{A}_p$ denote the row vector of amplitudes corresponding to the rows indexed by $C$: $\mathcal{A}_p = (\mathcal{A}_{j_1}, \ldots, \mathcal{A}_{j_M})$. Similarly let $\mathcal{A}_q$ be the row vector, the entries of which come from the complement of $C$: $\mathcal{A}_q = (\mathcal{A}_{k_1}, \ldots, \mathcal{A}_{k_{L-M}})$. One has

$$\text{E}[\mathcal{Z}_p] = e_1 C$$

$$\text{E}[\mathcal{Z}_q] = e_1 D$$

with

$$C = (\mathcal{V}^H R^{-1} \mathcal{V})^{1/2} \mathcal{A}_p$$

$$D = (\mathcal{V}^H R^{-1} \mathcal{V})^{1/2} \mathcal{A}_q.$$

Then

$$CC^H = (\mathcal{V}^H R^{-1} \mathcal{V}) \sum_{j \in C} |\mathcal{A}_j|^2 = (\mathcal{V}^H R^{-1} \mathcal{V}) \|\mathcal{A}_p\|^2 = \text{TASIR}_p$$

$$DD^H = (\mathcal{V}^H R^{-1} \mathcal{V}) \sum_{j \notin C} |\mathcal{A}_j|^2 = (\mathcal{V}^H R^{-1} \mathcal{V}) \|\mathcal{A}_q\|^2 = \text{TASIR}_q$$

where $\text{TASIR}_p$ ($\text{TASIR}_q$) is the ideal total array signal-to-interference ratio for the p-data (q-data). From Equation (D.4), $\text{TASIR} = \text{TASIR}_p + \text{TASIR}_q$.

The signal powers in the p-data and q-data can be identified with the averages $\|\mathcal{A}_p\|^2/L$ and $\|\mathcal{A}_q\|^2/L$. If $\mathcal{V}$ has unit norm and the noise floor has identity covariance, these averages are called, more precisely, *array signal-to-noise ratios* (ASNR) (see Section 4.1 for definitions; note that the noise floor covariance is denoted $R_N$ there).

## D.3.1 Detection

The detection statistics shown in the figures are essentially constant when the ideal TASIR of the SOI is large. A heuristic argument can be given to approximate this constant value.

Write the detection statistic as

$$\left(\frac{L-M}{M}\right)\lambda_{\max}(\mathcal{Z}_p^H \mathcal{S}^{-1}\mathcal{Z}_p) = \left(\frac{L-M}{M}\right)\lambda_{\max}(\mathcal{S}^{-1}\mathcal{Z}_p\mathcal{Z}_p^H).$$

The means of $\mathcal{Z}_p$ and $\mathcal{Z}_q$ can be written

$$
\begin{aligned}
\mathrm{E}[\mathcal{Z}_p] &= e_1(\mathcal{V}^H R^{-1}\mathcal{V})^{1/2}(A_{j_1},\ldots,A_{j_M}) = e_1(\mathcal{V}^H R^{-1}\mathcal{V})^{1/2}\mathcal{A}_p \\
\mathrm{E}[\mathcal{Z}_q] &= e_1(\mathcal{V}^H R^{-1}\mathcal{V})^{1/2}(A_{k_1},\ldots,A_{k_{L-M}}) = e_1(\mathcal{V}^H R^{-1}\mathcal{V})^{1/2}\mathcal{A}_q.
\end{aligned}
$$

When

$$\alpha \stackrel{\text{def}}{=} M^{-1}(\mathcal{V}^H R^{-1}\mathcal{V})\|\mathcal{A}_p\|^2 \gg 1,$$

one has

$$M^{-1}\mathcal{Z}_p\mathcal{Z}_p^H \approx \alpha e_1 e_1^H.$$

Unfortunately, a similar approximation is not always appropriate for $\mathcal{S}$. Define

$$\beta \stackrel{\text{def}}{=} (L-M)^{-1}(\mathcal{V}^H R^{-1}\mathcal{V})\|\mathcal{A}_q\|^2.$$

Let $\mathcal{S}_\rho$ be the random matrix obtained by replacing $(\mathcal{V}^H R^{-1}\mathcal{V})^{1/2}A_{k_l}$ with $\rho_l$, drawn from a set of independent identically distributed complex Gaussian random scalars with zero means and variances $\beta$. Then

$$(L-M)^{-1}(\mathcal{V}^H R^{-1}\mathcal{V})\|\mathcal{A}_q\|^2 = (L-M)^{-1}\mathrm{E}[\sum_l |\rho_l|^2] \approx (L-M)^{-1}\sum_l |\rho_l|^2$$

because, when $L-M \gg 1$, the right-hand side has a complex $\chi^2$ distribution that is tightly distributed about its mean. Then, because the distribution of $\mathcal{S}$ depends only on $(\mathcal{V}^H R^{-1}\mathcal{V})\|\mathcal{A}_q\|^2$, not on the specific vector $\mathcal{A}_q$,

$$(L-M)^{-1}\mathcal{S} \approx (L-M)^{-1}\mathcal{S}_\rho \approx (L-M)^{-1}\mathrm{E}[\mathcal{S}_\rho] = I_N + \beta e_1 e_1^H.$$

Finally,

$$\left(\frac{L-M}{M}\right)\lambda_{\max}(\mathcal{S}^{-1}\mathcal{Z}_p\mathcal{Z}_p^H) \approx \alpha\lambda_{\max}[(I_N + \beta e_1 e_1^H)^{-1}e_1 e_1^H] = \alpha/(1+\beta).$$

In the important case when $M = 1$, one can write, when $L \gg 1$,

$$\alpha/(1+\beta) = \frac{\text{TASIR}_p}{1 + \text{TASIR}_q/(L-1)} \approx L\frac{\text{TASIR}_p}{L + \text{TASIR}_q} \approx L\frac{\text{TASIR}_p}{\text{TASIR}_q}$$

where $\text{TASIR}_p$ and $\text{TASIR}_q$ are the total ASIRs in the p-data (which is now a single sample) and q-data. The final approximation holds when $\text{TASIR}_q \gg L$.

### D.3.2  False Alarm Statistic

This section discusses the false alarm statistic in the special case $J = 1 = M$. Aside from the first few paragraphs, it is self-contained; the notation used here is not necessarily related to the notation in the rest of this report.

The false alarm statistic can be expressed as $(J = 1 = M)$

$$\text{prob}\{L\,\mathcal{Z}_p^H \mathcal{S}^{-1} \mathcal{Z}_p \geq T\}.$$

The reason for introducing the factor $L$ will be apparent below. Recall that $\mathcal{Z}_p$ and $\mathcal{Z}_q$ (and hence $\mathcal{S} = \mathcal{Z}_q\mathcal{Z}_q^H$) are independent. Condition on the value of $\mathcal{Z}_p$ and choose a unitary $U$ so that $U\mathcal{Z}_p \propto e_1$. Then

$$\mathcal{Z}_p^H \mathcal{S}^{-1} \mathcal{Z}_p = (U\mathcal{Z}_p)^H (U\mathcal{S}U^H)^{-1}(U\mathcal{Z}_p) = \|\mathcal{Z}_p\|^2 (U\mathcal{S}U^H)^{11}$$

where, in general, $X^{ij}$ denotes the $(i,j)$th element of the inverse of $X$. But $U\mathcal{S}U^H$ and $\mathcal{S}$ have the same distribution (denoted $U\mathcal{S}U^H \sim \mathcal{S}$) because

$$\text{cov}(U\mathcal{Z}_q) = \text{cov}(\mathcal{Z}_q) = I_N \otimes I_{L-1}.$$

Thus

$$(U\mathcal{S}U^H)^{11} \sim \mathcal{S}^{11} \sim \frac{1}{\chi^2(L-N)} \tag{D.5}$$

where $\chi^2(L-N)$ is a complex $\chi^2$ random variable of degree $L-N$. Recall that, in general, $\chi^2(n)$ has the distribution of the sum $\sum_{k=1}^{n} \|z_k\|^2$ where the $\{z_k\}$ are independent complex circular Gaussians of zero mean and unit complex variance. The last equivalence in Equation (D.5) is a specific case of a well-known property of Wishart distributions (see, for example, Appendix 1 of Kelly and Forsythe [2]). Summarizing thus far, conditioned on $\mathcal{Z}_p$, one has

$$\mathcal{Z}_p^H \mathcal{S}^{-1} \mathcal{Z}_p \sim \frac{\|\mathcal{Z}_p\|^2}{\chi^2(L-N)}.$$

Because the denominator does not depend on the conditioning, one can write

$$\mathcal{Z}_p^H \mathcal{S}^{-1} \mathcal{Z}_p \sim \frac{\chi^2(N)}{\chi^2(L-N)}.$$

Recall that the incomplete beta function is defined

$$B(n,m,a) \stackrel{\text{def}}{=} \int_0^a t^{n-1}(1-t)^{m-1}\, dt$$

so that the complete beta comes

$$B(n,m) \stackrel{\text{def}}{=} B(n,m,1) = \frac{\Gamma(n)\Gamma(m)}{\Gamma(n+m)}.$$

Integrating by parts, one has

$$B(n,m,a) = \frac{a^n(1-a)^{m-1}}{n} + \frac{m-1}{n}B(n+1,m-1,a).$$

Iterating this leads to

$$B(n,m,a) = \sum_{k=0}^{m-1} \frac{(m-1)\cdots(m-k)}{n\cdots(n+k)} a^{n+k}(1-a)^{m-k-1}$$

so that

$$B(n,m)^{-1}B(n,m,a) = a^n(1-a)^{m-1} \sum_{k=0}^{m-1} \binom{n+m-1}{m-1-k}\left(\frac{a}{1-a}\right)^k \tag{D.6}$$

$$= a^{m+n-1} \sum_{k=0}^{m-1} \binom{n+m-1}{k}\left(\frac{1-a}{a}\right)^k. \tag{D.7}$$

41

The left-hand side of the above equation is the cumulative distribution function (CDF) of a complex $\beta(n, m)$ random variable (see Kelly and Forsythe [2] for a thorough discussion of the complex random variables introduced here). This random variable can be expressed in terms of a complex random variable $F(m, n)$ which, in turn, is the ratio of two independent, mean zero, complex $\chi^2$ random variables:

$$\beta(n, m) \sim \frac{1}{1 + F(m, n)}$$

$$F(m, n) \sim \frac{\chi^2(m)}{\chi^2(n)}.$$

Consider the false alarm probability for the detection statistic $(J = 1 = M)$

$$\text{prob}\{L F(N, L - N) \geq T\} = \text{prob}\{\beta(L - N, N) \leq \frac{1}{1 + T/L}\}.$$

Using Equation (D.7) one has, for large $L$ (which is the case of interest in the applications) the limiting behavior

$$\lim_{L \to \infty} \text{prob}\{L F(N, L - N) \geq T\} = e^{-T} \sum_{k=0}^{N-1} \frac{T^k}{k!}. \tag{D.8}$$

This expression provides the large $L$ false alarm behavior shown in the figures.

The false alarm probability can also be evaluated by employing a Chernoff bound. To do this, consider the moment generating function for the log of the beta random variable:

$$E[e^{\lambda \ln \beta(n, m)}] = B(n, m)^{-1} \int_0^1 t^{\lambda + n - 1} (1 - t)^{m-1} \, dt = \frac{B(\lambda + n, m)}{B(n, m)}$$

$$= \frac{\Gamma(\lambda + n)}{\Gamma(\lambda + n + m)} \cdot \frac{\Gamma(n + m)}{\Gamma(n)} = \prod_{k=0}^{m-1} \frac{n + k}{n + k + \lambda}.$$

Let $Q \stackrel{\text{def}}{=} \ln \frac{1}{1+T}$. Then

$$\text{prob}\{\beta(n, m) \leq \frac{1}{1 + T}\} = \text{prob}\{\ln \beta(n, m) \leq Q\}.$$

Define

$$f(\lambda) \overset{\text{def}}{=} \mathrm{E}[e^{\lambda(Q - \ln \beta)}] = e^{\lambda Q} \prod_{k=0}^{m-1} \frac{n+k}{n+k-\lambda}.$$

Chernoff's bound on the distribution tail is given by

$$\mathrm{prob}\{\ln \beta \leq Q\} \leq \inf_{\lambda \geq 0} \mathrm{E}[e^{\lambda(Q - \ln \beta)}] = \inf_{\lambda \geq 0} f(\lambda).$$

The derivative of $f(\lambda)$ is given by

$$f'(\lambda) = [Q + \sum_{k=0}^{m-1} \frac{1}{n+k-\lambda}] f(\lambda).$$

It is clear that the stationary points are relative minima. One can thus express the Chernoff bound parametrically as

$$Q(\lambda) = -\sum_{k=0}^{m-1} \frac{1}{n+k-\lambda} \tag{D.9}$$

$$f(\lambda) = e^{\lambda Q(\lambda)} \prod_{k=0}^{m-1} \frac{n+k}{n+k-\lambda} \tag{D.10}$$

$$T = e^{-Q(\lambda)} - 1. \tag{D.11}$$

A limiting form of the Chernoff bound is relevant for this report. Let $m = N$ and $n = L - N$ for the application to FFP. Further, replace $T$ with $T/L$ where $L \gg 1$. Then

$$\mathrm{prob}\{\beta(L - N, N) \leq \frac{1}{1 + T/L}\} \leq e^{\lambda Q(\lambda)} \prod_{k=0}^{N-1} \frac{L - N + k}{L - N + k - \lambda}$$

and

$$\lim_{L \to \infty} e^{\lambda Q(\lambda)} \prod_{k=0}^{N-1} \frac{L - N + k}{L - N + k - \lambda} = \left(\frac{eT}{N}\right)^N e^{-T}$$

43

when $T \geq N$, because $\lambda_{\min} \approx \frac{L(T-N)}{T}$ and $Q(\lambda) \approx -T/L$ (really, $\lambda_{\min}Q(\lambda_{\min}) \to N - T$ and $\lambda_{\min}/L \to 1 - \frac{N}{T}$).

Figure D-1 compares the asymptotic expressions and bounds discussed above to the true false alarm probability in one example. For this example, $L = 1000$ and $N = 4$. The Chernoff bound is given by the parametric expression above. The asymptotics of this expression are also shown. It is clear that the asymptotics of the incomplete beta [Equation (D.8)] are quite accurate; these asymptotics are used for Figure 3.

## D.4 Copy

Copy can be understood in terms of signal-to-interference ratios (SIR). This section considers very general notions of SIRs based on the estimate of the parameters $A$. These SIRs are specialized to FFP applications in a subsection.
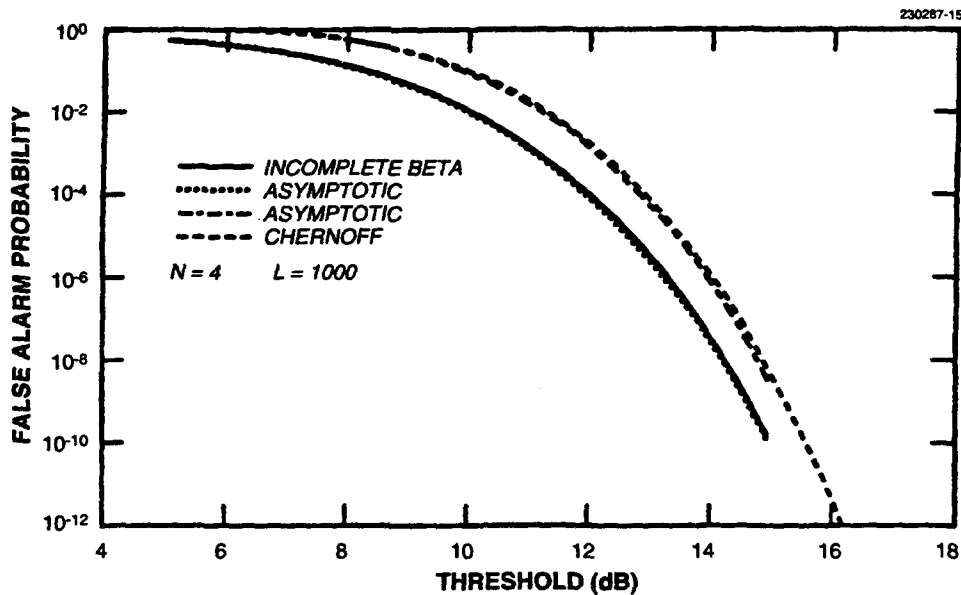


*Figure D-1. Comparison of Incomplete Beta function, bounds, and asymptotics.*

Some additional notation is required. Define the $JK$ column vector $\text{Vec}(X)$ of the $J \times K$ matrix $X$ so that

$$X_{jk} = (\text{Vec}(X))_{(j-1)K+k}.$$

Some properties of Vec are easily verified for arbitrary matrices (with conformal dimensions) $X, Y, C, D$:

1. $\text{Vec}(X)^H \text{Vec}(Y) = \text{tr}(X^H Y)$

2. $(C \otimes D)\text{Vec}(X) = \text{Vec}(CXD^T)$

3. $\text{Vec}(Y)^H (C \otimes D)\text{Vec}(X) = \text{tr}(Y^H CXD^T)$ .

Recall that Kronecker products are defined in Section A.1. The ML estimate $\hat{A}$ of the signal amplitudes $\mathcal{A}$ is given by

$$\hat{A} = W^H Z T^H (TT^H)^{-1} = (W \otimes \overline{T^H(TT^H)^{-1}})^H \text{Vec}(Z). \tag{D.12}$$

Thus one can view both $W$ and $T$ as weights. To form $W$, one needs an estimate $\hat{V}$ of $\mathcal{V}$, provided by

$$\hat{V} = e_J(Z_p Z_p^H S^{-1})\Theta$$

where $e_J(\cdot)$ denotes the $N \times J$ array formed by the top $J$ eigenvectors of its argument. Only the column span of $e_J$ is unique. The ambiguity is expressed by the post-factor $\Theta$, which changes bases for the column space. Because, in general,

$$W = S^{-1}\hat{V}(\hat{V}^H S^{-1}\hat{V})^{-1},$$

one has

$$W = e_J(S^{-1}Z_p Z_p^H)\Theta.$$

Again, the postfactor $\Theta$ (different each time) expresses nonuniqueness. Define

$$\mathcal{W} \overset{\text{def}}{=} UR^{1/2}W = e_J(\mathcal{S}^{-1}\mathcal{Z}_p \mathcal{Z}_p^H)\Theta.$$

Ideally, one would characterize the estimate $\hat{A}$ by providing distributional information, or failing that, first and second moment information. A less ambitious, but physically reasonable approach is taken here. In this approach $W$ (and hence $\mathcal{W}$) is assumed constant in the calculation of a SIR based on first and second moments of $\hat{A}$. Then the statistical behavior of $W$ is introduced to characterize this SIR as a random variable. This makes sense if, for example, the data used to determine $W$ (and $T$) and the data used in Equation (D.12) are independent. Then, using the properties of Vec described above and the properties of covariance described in Section 2.1, one can write

$$\text{cov}_W(\hat{A}) = (W^H R W) \otimes \overline{(TT^H)}^{-1} = (\mathcal{W}^H \mathcal{W}) \otimes \overline{(TT^H)}^{-1}.$$

In addition,

$$\begin{aligned}
\text{Vec}(\text{E}_W[\hat{A}]) &= \text{Vec}[W^H \mathcal{V}\mathcal{A}(TT^H)(TT^H)^{-1}] = \text{Vec}[W^H E_J \mathcal{B}\Gamma(TT^H)^{-1/2}] \\
&= (\mathcal{W} \otimes \overline{(TT^H)}^{-1/2})^H \text{Vec}[E_J \mathcal{B}\Gamma].
\end{aligned}$$

These "mean" and "covariance" statistics are based on a fixed value of $W$; hence the $W$ subscripts.

One can define a random variable called the achieved TASIR as follows:

$$\max_X \frac{|X^H \text{Vec}(\text{E}_W[\hat{A}])|^2}{X^H \text{cov}_W(\hat{A}) X} = \text{Vec}(\text{E}_W[\hat{A}])^H \text{cov}_W(\hat{A})^{-1} \text{Vec}(\text{E}_W[\hat{A}]).$$

Upon using the properties of the Kronecker product and of Vec, this becomes

$$\begin{aligned}
&\text{Vec}(E_J \mathcal{B}\Gamma)^H (\mathcal{W}(\mathcal{W}^H \mathcal{W})^{-1} \mathcal{W}^H \otimes I_M) \text{Vec}(E_J \mathcal{B}\Gamma) \\
&= \text{Vec}(\mathcal{B})^H [(E_J^H \mathcal{W}(\mathcal{W}^H \mathcal{W})^{-1} \mathcal{W}^H E_J) \otimes (\Gamma\Gamma^H)^T] \text{Vec}(\mathcal{B}) \\
&= \text{tr}[\mathcal{B}^H E_J^H \mathcal{W}(\mathcal{W}^H \mathcal{W})^{-1} \mathcal{W}^H E_J \mathcal{B}\Gamma\Gamma^H] \\
&= \text{tr}[E_J^H \mathcal{W}(\mathcal{W}^H \mathcal{W})^{-1} \mathcal{W}^H E_J C C^H]
\end{aligned}$$

where $C$ is defined in Section D.1.

Note that $\mathcal{W}(\mathcal{W}^H \mathcal{W})^{-1} \mathcal{W}^H$ depends only on the column space of $\mathcal{W}$, because it is the orthogonal projector onto that subspace. Furthermore, the argument of Section D.2 shows that the distribution of this projector only depends on the dimensional parameters $N$, $M$, $J$, $L$, and on the signal levels expressed through $CC^H$ and $DD^H$. Because the projector is the only random variable in the achieved TASIR expression above, this is the desired normal form for copy performance.

46

More generally, one is interested in the SIR based on

$$W^H Z \tilde{T}^H (\tilde{T} \tilde{T}^H)^{-1},$$

where $W$ (and $T$) are determined as above, but the $\mathcal{M} \times L$ array $\tilde{T}$ "selects" a different part of $\mathcal{A}$ (see special case below). Defining $\tilde{C}$ so that

$$\tilde{C} \tilde{C}^H = (\mathcal{V}^H R^{-1} \mathcal{V})^{1/2} [\mathcal{A} \mathcal{T} (\tilde{T}^H (\tilde{T} \tilde{T}^H)^{-1} \tilde{T}) \mathcal{T}^H \mathcal{A}^H] (\mathcal{V}^H R^{-1} \mathcal{V})^{1/2}, \qquad \text{(D.13)}$$

the calculation above yields an achieved TASIR given by

$$\text{tr}[E_J^H \mathcal{W} (\mathcal{W}^H \mathcal{W})^{-1} \mathcal{W}^H E_J \tilde{C} \tilde{C}^H].$$

As before, $\mathcal{W}$ depends only on the dimensional parameters, $CC^H$, and $DD^H$.

The reason for the more general SIR is that the weights $W$ and $T$ may be determined by only part of the signal (the spectral lines in FFP applications) but copy performance may be required on a different part.

### D.4.1 Special Case

Recalling the expression for $\tilde{C} \tilde{C}^H$ above, when $J = 1$, the achieved TASIR becomes

$$(e_1^H \mathcal{W} (\mathcal{W}^H \mathcal{W})^{-1} \mathcal{W}^H e_1) (\mathcal{V}^H R^{-1} \mathcal{V}) (\mathcal{A} \mathcal{T} \tilde{T}^H (\tilde{T} \tilde{T}^H)^{-1} \tilde{T} \mathcal{T}^H \mathcal{A}^H)$$

$$= (e_1^H \mathcal{W} (\mathcal{W}^H \mathcal{W})^{-1} \mathcal{W}^H e_1) (\mathcal{V}^H R^{-1} \mathcal{V}) \sum_{k \in \tilde{C}} |\mathcal{A}_k|^2,$$

where $\tilde{T} = \mathcal{T}_{\tilde{C}}$ (see Section D.3 for notation). The first factor expresses the loss due to sampling (including suppression effects due to mismatch, as expressed by $DD^H$). The second factor (if $\mathcal{V}$ has unity norm) expresses the loss of SIR due to the spatial distribution of interference, and the last factor is the signal energy in the subband expressed by the set $\tilde{C}$. It is important to note that the loss factor is common to all SIR expressions, no matter what part $\tilde{C}$ of the signal is used to assess copy. In the particular case when $\tilde{C} = C$, the above can be written

$$(e_1^H \mathcal{W} (\mathcal{W}^H \mathcal{W})^{-1} \mathcal{W}^H e_1) \text{TASIR}_T.$$

Of course, the achieved ASIR, which is defined on a per look basis, is always smaller by a factor of $L$.

# REFERENCES

1. E.J. Kelly, "An Adaptive Detection Algorithm," *IEEE Trans. Aerospace Electronics and Systems*, 115–127, (1986).

2. E.J. Kelly and K.W. Forsythe, "Adaptive Detection and Parameter Estimation for Multidimensional Signal Models," Massachusetts Institute of Technology Lincoln Laboratory, Lexington, Mass., Technical Report 848 (April 1989). DTIC ADA208971.

3. G. Golub and C. Van Loan, *Matrix Computations*, Baltimore, Maryland: Johns Hopkins University Press (1983).

4. R. Bellman, *Introduction To Matrix Analysis*, New York, New York: McGraw-Hill (1960).

5. R.A. Horn and C.R. Johnson, *Matrix Analysis*, Cambridge, Mass.: Cambridge University Press (1988).

6. D. Delong, "Use of the Weiss-Weinstein Bound to Compare the Direction-Finding Performance of Sparse Arrays," Massachusetts Institute of Technology Lincoln Laboratory, Lexington, Mass., Technical Report 982 (1993). DTIC ADA272582.

# REPORT DOCUMENTATION PAGE

| 1. AGENCY USE ONLY (Leave blank) | 2. REPORT DATE 20 June 1994 | 3. REPORT TYPE AND DATES COVERED Technical Report |
|---|---|---|

**4. TITLE AND SUBTITLE**

Adaptive Detection and Copy of Coherent Narrowband Waveforms
with Uncalibrated Arrays

**5. FUNDING NUMBERS**

C — F19628-90-C-0002

**6. AUTHOR(S)**

Keith W. Forsythe

**7. PERFORMING ORGANIZATION NAME(S) AND ADDRESS(ES)**

Lincoln Laboratory, MIT
P.O. Box 73
Lexington, MA 02173-9108

**8. PERFORMING ORGANIZATION REPORT NUMBER**

TR-994

**9. SPONSORING/MONITORING AGENCY NAME(S) AND ADDRESS(ES)**

HQ Electronic Systems Center ESC/ENKL
Hanscom AFB, MA 01730-5000

**10. SPONSORING/MONITORING AGENCY REPORT NUMBER**

ESC-TR-93-292

**11. SUPPLEMENTARY NOTES**

None

**12a. DISTRIBUTION/AVAILABILITY STATEMENT**

Approved for public release; distribution is unlimited.

**12b. DISTRIBUTION CODE**

**13. ABSTRACT (Maximum 200 words)**

Adaptive detection and copy of temporally coherent narrowband waveforms with multiple sensors is discussed. Unlike related problems treated in the radar literature, the sensor response to the coherent signal of interest is assumed unknown. Thus the techniques presented can be used with uncalibrated sensor arrays. The signal processing takes advantage of the sensor array as well as the signal coherence in order to form an adaptive spatial beam that suppresses cochannel interference. More general signal models involving partial coherence are also considered.

**14. SUBJECT TERMS**

adaptive antenna array
generalized likelihood ratio
maximum likelihood
radar
detection
beamforming
spectrum estimation

**15. NUMBER OF PAGES**
60

**16. PRICE CODE**

| 17. SECURITY CLASSIFICATION OF REPORT | 18. SECURITY CLASSIFICATION OF THIS PAGE | 19. SECURITY CLASSIFICATION OF ABSTRACT | 20. LIMITATION OF ABSTRACT |
|---|---|---|---|
| Unclassified | Unclassified | Unclassified | Same as Report |